Liquid Crystals
Publication details, including instructions for authors and subscription information:
http://www.informaworld.com/smpp/title~content=t713926090

Magnetic field induced bistability in nematics and cholesterics: general deformations

U. D. Kini[a]
[a] Raman Research Institute, Bangalore, India

To cite this Article Kini, U. D.(1992) 'Magnetic field induced bistability in nematics and cholesterics: general deformations', Liquid Crystals, 12: 3, 449 — 475
To link to this Article: DOI: 10.1080/02678299208031061
URL: http://dx.doi.org/10.1080/02678299208031061

LIQUID CRYSTALS, 1992, VOL. 12, NO. 3, 449–475

Magnetic field induced bistability in nematics and cholesterics: general deformations

by U. D. KINI
Raman Research Institute, Bangalore-560080, India

(*Received 2 August 1991; accepted 28 January 1992*)

The continuum theory is used for studying magnetic field (**H**) induced orientational bistability of the director field (**n**) of a nematic with positive diamagnetic susceptibility anisotropy (χ_a) the nematic being confined between two plane parallel plates. The rigid anchoring hypothesis is utilized for investigating the effect of variation of magnetic tilt on the nature of change of director deformation described by two distortion angles. Such general deformations can result, for instance, when **H** is slowly rotated in a plane whose normal does not coincide with the normal to the sample planes. The bistability width w_b (the range of magnetic tilt angle over which two different equilibrium configurations can exist) depends upon various parameters such as the elastic ratios, the angle of inclination of **n** at the boundaries and the twist in the ground state. In particular, the nature of change of distortion exhibits certain new features when **n** is pretilted at the sample boundaries. Scaling analysis indicates that w_b should be independent of the sample thickness at a given reduced field. Linear time dependent perturbation analysis shows that where bistability is associated with discontinuous orientational change, the static deformation is susceptible to instability near the edges of the bistable region. Scaling analysis of the general dynamical equations indicates that even at the same reduced field we cannot rule out a strong dependence of the time of transition between deformation states on sample thickness. When the nematic has $\chi_a < 0$, a threshold magnetic tilt may exist separating two different types of distortion; this is indicated by the time independent perturbation analysis. The possible effects of an additional electric field are briefly discussed. In the light of recent experimental evidence it seems interesting to generalize the rotating field (or sample) experiments discussed in an earlier paper.

1. Introduction

Various static and dynamic effects resulting from the application of magnetic (**H**) and electric (**E**) fields on nematic and cholesteric liquid crystals have been satisfactorily explained by the continuum theory [1–8] which assigns a non-polar unit director vector field **n** to describe the preferred direction of molecular orientation. Owing to the anisotropic susceptibilities of these materials, **E** or **H** can produce torques which tend to change **n**. Due to the anchoring effects of the sample boundaries the field induced orienting torques give rise to spatial gradients of **n** which, in turn, produce curvature elastic restoring torques. Under the combined action of these torques the sample attains an equilibrium configuration corresponding to some total free energy. A change in the external field causes the fluid to reach a different equilibrium state with a different free energy. The difference in free energy is dissipated by transient viscous effects which result from the time rate of change of **n** as the sample goes over from one equilibrium configuration to another. Many interesting viscoelastic effects arise out of the anisotropic couplings between **n** and the transient flow (see, for instance, [9, 10]).

0267–8292/92 $3·00

When **H** is applied along the uniform orientation direction ($\mathbf{n}_0$) of a nematic sample with $\chi_a > 0$, **H** acts as a stabilizing field. When **H** is impressed at some arbitrary angle with respect to $\mathbf{n}_0$, a monodomain homogeneous deformation eventually sets in; such a distortion is uniform in the sample plane but varies only along the sample normal. When **H** is applied normal to $\mathbf{n}_0$ a deformation sets in only when $H > H_F$, the Freedericksz threshold; above the threshold homogeneous distortions of opposite parity can form, separated by domain walls. In the light of these facts it should be interesting to find out how the deformation changes when **H** is slowly rotated away from $\mathbf{n}_0$ or $-\mathbf{n}_0$, with the axis of rotation being normal to $\mathbf{n}_0$. This problem can be treated under statics by neglecting transient dissipative processes which arise every time the magnetic angle (say α) is changed.

This was first attempted, theoretically and experimentally, by Onnagawa and Miyashita [11]. Using capacitance measurements they showed that when $H < H_F$, the distortion changes continuously with α without exhibiting bistability (we shall call this type A behaviour) while, when $H > H_F$, the deformation exhibits bistability and changes discontinuously when α exceeds a critical value (type B behaviour) resulting in hysterisis for reversal of the direction of change of α. Subsequently, Motooka and Fukuhara [12] extended the theoretical analysis of [11] to show that there can exist two stable configurations with different free energy over certain ranges of α when H is sufficiently high. In this case it is possible to expect type B behaviour.

Recently, Karn and Shen [13] studied **H** induced bistability in a homeotropically anchored nematic (**n** anchored normal to the sample planes). Using optical observations they studied the variation of bistability width w_b as a function of **H** to obtain results in qualitative agreement with those of [11, 12]. They also measured the time rate of change of deformation near the edges of the bistable region and interpreted their results using the continuum theory to obtain good quantitative agreement with the measured time of transition τ_R.

In a recent attempt [14] bistability has been studied by generalizing the previous theoretical work to include different ground states and suitable magnetic planes. Bistability is found to occur even in situations where a Freedericksz threshold cannot be defined. Director anchoring strengths at the boundaries [15] as well as an additional **E** can greatly influence w_b. For rigid anchoring, however, scaling analysis indicates that w_b should depend only on the reduced field (H/H_F) while τ_R should strongly depend on the sample thickness. Linear perturbation analysis shows that the static type B solution has a propensity towards instability near the edges of the bistable region. Considering the variety of results already obtained (see, for example, [16–20]) it seems meaningful to generalize the static case to include dynamic effects induced by a uniformly rotating **H** or sample.

All the above efforts have considered configurations with **n** described by a single distortion angle and **H** by a single angle of tilt. As **n** is a unit vector it can, in general [21], be specified by two angles. It should be instructive to find out how w_b is affected when **n** and **H** are both described by two degrees of freedom each. In such cases the dynamics will be more general with velocity gradients being invariably coupled to **n**. It should also be instructive to find out how scaling and perturbation analyses are likely to be affected. The case of weak anchoring should apply more generally as both anchoring strengths may enter the picture. If the material is a cholesteric then the amount of intrinsic twist may also affect the occurrence of bistability.

With this motivation the governing equations are derived and the boundary conditions specified in § 2. Section 3 contains results on bistability based on the static

part of the theory. In § 4 the dynamical equations are set up and solved in the linear limit to shed some light on the stability of the static solution against imposed perturbations. Section 5 concludes the discussion.

2. Governing equations, boundary conditions and method of solution

It is convenient to adopt the procedure of [21] with some variation. Consider a cholesteric confined between plane parallel plates $z = \pm h$ (sample thickness $= 2h$) at which the easy directions of anchoring are given by

$$d_\pm = (\cos\theta_\pm \cos\phi_\pm, \cos\theta_\pm \sin\phi_\pm, \sin\theta_\pm) \tag{2.1}$$

in rectangular cartesian coordinates. A field

$$\mathbf{H} = (HC_\alpha C_\beta,\ HC_\alpha S_\beta,\ HS_\alpha); \quad C_\alpha = \cos\alpha; \quad S_\beta = \sin\beta \tag{2.2}$$

is impressed on the sample. The angles α and β can be referred to as the magnetic polar and azimuthal angles, respectively. The resulting homogeneously deformed configuration is taken to be

$$\mathbf{n} = (C_\theta C_\phi,\ C_\theta S_\phi,\ S_\theta); \quad \theta = \theta(z); \quad \phi = \phi(z). \tag{2.3}$$

Using (2.2) and (2.3), the deformation dependent part of the total free energy density

$$\left.\begin{aligned} W_V &= f_1(\theta)\phi_{,z} + [\{f_2(\theta)\theta_{,z}^2 + f_3(\theta)\phi_{,z}^2\}/2] + f_4(\theta,\phi); \\ f_1(\theta) &= -k_2 C_\theta^2; \quad f_2(\theta) = K_1 C_\theta^2 + K_3 S_\theta^2; \quad f_3(\theta) = K_2 C_\theta^4 + K_3 S_\theta^2 C_\theta^2; \\ f_4(\theta,\phi) &= -\mu_0 \chi_a H^2 [C_\alpha C_\theta \cos(\beta-\phi) + S_\alpha S_\theta]^2/2, \end{aligned}\right\} \tag{2.4}$$

where K_1, K_2, K_3 are the splay, twist and bend elastic constants, respectively; $k_2 = 2\pi K_2/P_0$; P_0 is the equilibrium pitch of the cholesteric; $\phi_{,z} = d\phi/dz$, etc. For a nematic, $k_2 = 0$. The surface free energy density is [15]

$$W_S(z = \pm h) = [B_{\theta\pm} \sin^2(\theta - \theta_\pm) + B_{\phi\pm} \sin^2(\phi - \phi_\pm)]/2, \tag{2.5}$$

where $B_{\theta\pm}$, $B_{\phi\pm}$ are the splay and twist anchoring strengths, respectively, at $z = \pm h$. Minimizing the free energy the following governing equations and boundary conditions result:

$$\left.\begin{aligned} \Gamma_\theta &= f_2(\theta)\theta_{,zz} + [(df_2/d\theta)\theta_{,z}^2 - (df_3/d\theta)\phi_{,z}^2]/2 - (\partial f_4/\partial\theta) - (df_1/d\theta)\phi_{,z} = 0; \\ \Gamma_\phi &= f_3(\theta)\phi_{,zz} + (df_1/d\theta)\theta_{,z} + (df_3/d\theta)\theta_{,z}\phi_{,z} - (\partial f_4/\partial\phi) = 0; \end{aligned}\right\} \tag{2.6}$$

$$\left.\begin{aligned} &[f_2(\theta)\theta_{,z} \pm B_{\theta\pm} \sin(\theta - \theta_\pm)\cos(\theta - \theta_\pm)](z = \pm h) = 0; \\ &[f_1(\theta) + f_3(\theta)\phi_{,z} \pm B_{\phi\pm} \sin(\phi - \phi_\pm)\cos(\phi - \phi_\pm)](z = \pm h) = 0. \end{aligned}\right\} \tag{2.7}$$

When the anchoring at the walls is not rigid there is restriction, shown by these expressions mainly on the spatial derivatives θ and ϕ at the sample boundaries; the orientation of $\mathbf{n}$ can deviate from the easy direction (see equation (2.1)). Interestingly, in the present case both splay and twist anchoring strengths enter the picture while only one of them figures in the situations [14] where $\mathbf{n}$ is described by only one angle. If the anchoring is rigid then

$$\theta(z = \pm h) = \theta_\pm; \quad \phi(z = \pm h) = \phi_\pm. \tag{2.8}$$

Except when the easy axes (see equation (2.1)) and the magnetic tilt (see equation (2.2)) assume special values, the equations (2.6) are always coupled. Thus, in general,

any change in $\theta(z)$ will affect $\phi(z)$ and vice versa. The presence of cross coupling terms such as $(df_3/d\theta)\theta_{,z}\phi_{,z}$ must also be kept in mind. These essentially couple $\theta(z)$ and $\phi(z)$. The presence of such a mechanism can lead to strikingly different behaviour in the present case as compared to situations [11–14] where **n** depends on a single angle.

For the given set of parameters and boundary orientations, equations (2.8) and (2.6) are solved numerically using the orthogonal collocation method [22] with the zeros of the 24th order Legendre polynomial being used as collocation points [23]. Once the $\theta(z)$ and $\phi(z)$ profiles have been found, the total volume free energy F can be computed by gaussian quadrature integration [23] of W_V from equation (2.4) over the sample assuming some convenient areas of the boundary planes. Equations (2.6) and (2.8) are valid for cholesterics as well as for nematics. For the sake of simplicity we shall consider only nematics in the present work ($k_2=0$). In § 5 a brief qualitative discussion is presented regarding additional effects which might be associated with chiral nematics.

In some cases $\theta(z)$ and $\phi(z)$ turn out to be symmetric with respect to the sample centre where they assume maximum values, θ_m, ϕ_m, respectively. It is then natural to use θ_m and ϕ_m to characterize the distortion. It is found that $\theta(z=0)$ and $\phi(z=0)$ generally provide a convenient measure of deformation even in cases where the distortion is asymmetric. It is the aim of the next section to examine how deformation and F vary with magnetic tilt.

The sample thickness is assumed to be $2h=200\,\mu$m for calculations. In most cases this does not explicitly come into the picture as will be seen presently. Angles are measured in radians. The material parameters used are [24]

$$(K_1,K_2,K_3)=(1{\cdot}85,\ 1{\cdot}3,\ 2{\cdot}02)\times 10^{-12}\ \text{N}. \tag{2.9}$$

A convenient value of 10^{-6} (SI) is chosen for χ_a. This value is again immaterial as the final results are discussed in terms of a reduced field. In this work, χ_a is assumed to be positive unless otherwise stated.

3. Results in the static limit—bistability and discontinuous orientational changes

Various kinds of ground state (configuration of **n** in the absence of **H**) can be studied with equation (2.1). With $\phi_\pm=0$ and $\theta_\pm=\theta_1$ one gets a uniform **n** in the xz plane tilted at an angle θ_1 to the x axis; with $\theta_1=0$ and $\phi_\pm=\pm\phi_0$ (without loss of generality) the ground state is uniformly twisted with a total twist of $2\phi_0$ which may exceed $\pi/2$ for cholesterics or chiral nematics but not a simple twisted nematic. For non-zero values of $\theta_\pm$ and ϕ_0 it is possible to think of more general ground states (see, for instance, [25]).

To obtain a complete picture of the variation of distortion with magnetic tilt it is advisable to keep one of the tilt angles (α or β) fixed and vary the other (β or α). To find out the possible ranges of variation of α or β, it is necessary to study some of the symmetries of equations (2.6) and (2.8), i.e. transformations which leave the solution unchanged. For instance,

$$\alpha\rightarrow\alpha+\pi, \tag{3.1}$$

$$\beta\rightarrow\beta+\pi;\quad \alpha\rightarrow\pi-\alpha, \tag{3.2}$$

are generally valid due to the non-polarity of **n**.

3.1. $\phi_\pm = 0$; $\theta_\pm = 0$; $k_2 = 0$

The ground state is homogeneously aligned along the x axis. As the boundary conditions are symmetric, $\theta(z)$,$\phi(z)$ will also be symmetric and assume extremum values θ_m, ϕ_m, respectively, at the sample centre. In this case additional symmetry transformations also result. For example,

$$\alpha \rightarrow \pi - \alpha; \quad \theta \rightarrow -\theta \tag{3.3}$$

leaves equations (2.6) and (2.8) unchanged. In addition it is seen that $\beta = (\pi/2) \pm \beta_1$ are equivalent provided that

$$\phi \rightarrow -\phi; \quad \alpha \rightarrow \pi - \alpha. \tag{3.4}$$

This means that we can fix the following ranges for the variation of α:

$$0 \leqq \alpha \leqq \pi; \quad 0 \leqq \beta \leqq \pi/2. \tag{3.5}$$

It is next necessary to fix a characteristic field to measure H. When $\beta = 0$, a variation of α results in **H** being rotated in the xz plane. Then $\phi(z) = 0$. It is natural to choose $H_F = (\pi/2h)(K_1/\mu_o\chi_a)^{1/2}$, the splay Freedericksz threshold, as a measure of H. When $\beta = \pi/2$ and α is varied, **H** rotates in the yz plane. This is the oblique field configuration [6] in which $\theta(z)$ and $\phi(z)$ appear above a threshold

$$H_o(\alpha) = (\pi/2h)\,[K_1K_2/\{\mu_o\chi_a(K_2S_\alpha^2 + K_1C_\alpha^2)\}]^{1/2}, \tag{3.6}$$

which is itself a function of α. It seems convenient, therefore, to use H_F as the characteristic field.

Figure 1 shows plots of θ_m and ϕ_m as functions of the magnetic polar angle α for different values of the magnetic azimuthal angle β. Figure 2 depicts the variation of the total free energy F versus α for a few representative cases. The nature of variation of θ_m and ϕ_m with α is found to depend on the reduced field $R = H/H_F$ and β. For a given β, ϕ_m varies in the range $-\beta < \phi_m < \beta$. For any value of β, ϕ_m crosses zero as α passes through $\pi/2$. This is clearly because **H** will be directed along the z axis when $\alpha = \pi/2$ regardless of the value of β; there can then be only a $\theta(z)$ distortion and $\phi(z)$ must vanish throughout the sample. It may be noted that the variations of θ_m and ϕ_m are in conformity with equation (3.3).

When β is small ($= 0{\cdot}01$; see figures 1 (*a*) and (*b*)), **H** rotates close to the xz plane. The dominant distortion is $\theta(z)$, ϕ_m being very small. When H is low enough, the deformation is type A (curves 1 and 2). When $R > 1$, however, one finds the type B variation (curves 3) with bistability (dashed lines are used to mark bistable regions). A discontinuous transition at the edge of the bistable region from a higher energy state on one branch to the corresponding lower energy state on the other branch cannot be ruled out. The nature of variation of θ_m is similar to that studied in earlier work [11–14] for the single angle deformations.

When β is enhanced ($= 0{\cdot}78$; see figures 1 (*c*) and (*d*)) the curves are similar to those of figures 1 (*a*) and (*b*), except that the bistability width w_α for $R > 1$ is considerably greater than that at $\beta = 0{\cdot}01$. When β is further augmented ($= 1{\cdot}17$; see figures 1 (*e*) and (*f*)) the nature of distortion change becomes somewhat different from the earlier cases. At low fields ($R \leqq 1$) we find the type A variation. At a higher field ($R = 1{\cdot}5$; curves 3) the deformation changes continuously over the entire π range of α, exhibiting bistability; this is a new kind of variation which we shall call type C. In a small range of intermediate field strengths, $1{\cdot}0 < R < 1{\cdot}4$, we again find the type B behaviour.

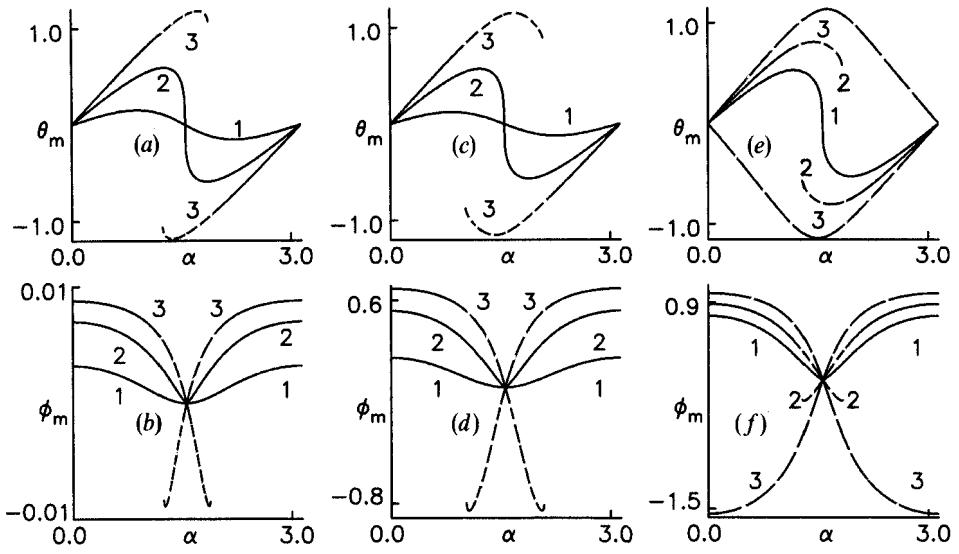

Figure 1. Variation of θ_m and ϕ_m as functions of the magnetic polar angle α for different values of the reduced field $R=H/H_F$ and magnetic azimuthal angle β. H_F is the splay Freedericksz threshold. The ground state is homogeneously oriented along x; $(\theta_\pm=\theta_1=0)$. The director is rigidly anchored at the boundaries. Under the action of **H** from equation (2.2), **n** gets distorted such that $\theta(z)$, $\phi(z)$ are symmetric with respect to the sample centre $z=0$; $\theta_m=\theta(z=0)$ and $\phi_m=\phi(z=0)$ are the maxima of the deformation angles. Material parameters are as in equation (2.9). $\beta=(a)$, (b) 0·01 (c), (d) 0·78 (e), (f) 1·17 rad. Curves have been drawn for $R=(1)$ 0·5 (2) 1·0 (3) 1·5 in (a)–(d). $R=(1)$ 1·0 (2) 1·2 (3) 1·5 in (e) and (f). Dashed lines represent regions of bistability. Depending upon the values of β and R, we can find behaviour of type A, B or C; when **n** and **H** are confined to the same plane [11–14] it is possible to find only deformation variation of types A and B. A qualitative explanation in terms of energetics can be found in § 3.1.

The above results can be described qualitatively as follows. When R is small enough the dominance of elastic torque over the magnetic torque ensures that the distortion does not grow beyond a certain limit. As there can be no deformation at $\alpha=\pi/2$ for $R\leqq 1$ (or, equivalently, for $H\leqq H_F$), both θ_m and ϕ_m must pass through zero as α crosses $\pi/2$; this must hold for any value of β. When $R>1$ the $\theta(z)$ (splay–bend) distortion increases as α is varied from 0 or π. Because $R>1$, θ_m does not become zero as α crosses $\pi/2$. When β is small the entire distortion is almost purely splay–bend and confined to the xz plane as $\chi_a>0$. There is no scope for a twist $\phi(z)$ to build up sufficiently to drain off free energy from the splay–bend component (we remember that $|\phi_m|<\beta$ and that β is small). In this case when α is varied beyond $\pi/2$, θ_m increases further making an energetically stable solution impossible when α crosses a critical angle α_0 (which we identify as the edge of the bistable region). This causes the type B distortion to be described by two distinct branches $(0\leqq\alpha\leqq\alpha_0;\ \pi-\alpha_0\leqq\alpha\leqq\pi)$ having an overlapping region of bistability which extends symmetrically about $\alpha=\pi/2$ over the bistability width $w_\alpha=2\alpha_0-\pi$. Any attempt to vary α beyond the edge of any one branch results in the configuration changing irreversibly to the corresponding low energy state on the other branch; such transitions have been experimentally observed [11, 13].

When β is sufficiently high and α close to 0 or π, the distortion is predominantly twist. The splay–bend component develops only as α is varied towards $\pi/2$. When $R>1$

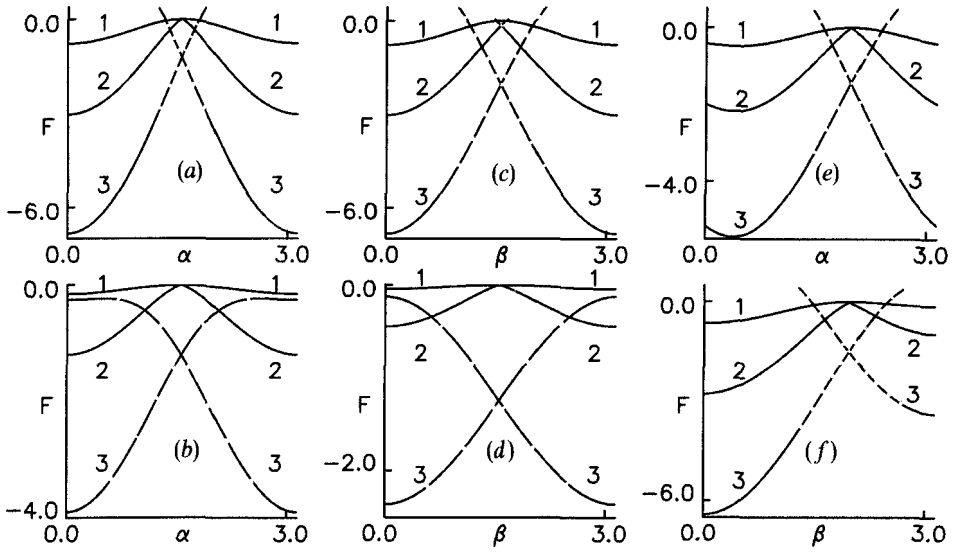

Figure 2. Variation of the total free energy F (units 10^{-10} J) as a function of the magnetic tilt angles at different R for rigid anchoring. Compare with figures 1 and 3. In (*a*)–(*d*) the ground state is homogeneous along x ($\theta_1 = 0$). F versus α for $\beta =$ (*a*) 0·01 (*b*) 1·17. $R =$ (1) 0·5 (2) 1·0 (3) 1·5 in (*a*) $R =$ (1) 0·5 (2) 1·2 (3) 1·5 in (*b*) F versus β for $\alpha =$ (*c*) 0·01 (*d*) 1·36. $R =$ (1) 0·5 (2) 1·0 (3) 1·5 in (*c*) and (*d*). It is instructive to compare (*b*) and (*d*) with (*a*) and (*c*), respectively. For type C variation of distortion, F near the centre of the magnetic tilt range is generally lower than F for type B variation (see § 3.1). (*e*) and (*f*) ground state is tilted in the xz plane at $\theta_\pm = \theta_1$ with the x axis. (*e*) $\theta_1 = 0{\cdot}78$; $\beta = 1{\cdot}17$. F versus α at $R =$ (1) 0·5 (2) 1·0 (3) 1·5. (*f*) $\theta_1 = 0{\cdot}39$; $\alpha = 0{\cdot}78$. F versus β at $R =$ (1) 0·5 (2) 1·0 (3) 1·5. The strong asymmetry in the variation of F with respect to the centre of the magnetic tilt range should be noted. This is due to the different ways in which splay–bend couples with twist when the magnetic tilt is varied from the opposite ends of its range for non-zero director pretilt at the sample boundaries (see § 3.3).

and α reaches $\pi/2$, $|\theta_m|$ is maximum and $\phi_m = 0$. Suppose H is sufficiently high. Then when α is varied beyond $\pi/2$ in the same direction, **H** tends to pull **n** out of the xz plane via a twist. This means an increase in $|\phi_m|$ which can only be at the expense of $|\theta_m|$; as the twist component in the deformation gets augmented, the splay–bend component diminishes. Thus when R is sufficiently high the deformation change is of type C—a continuous variation along two different paths over the entire π range when α is varied from the two ends of its range. When this behaviour is contrasted with the type A variation expected for low R (no bistability but continuous variation of deformation) it is immediately clear that when β is high enough the nature of distortion change must be of type B over some intermediate range of R.

Some of these points become clear when we compare the curves of total free energy F versus α for different β and R (see figures 2 (*a*) and (*b*)). It is seen that for $\beta = 1{\cdot}17$, F remains lower than that for $\beta = 0{\cdot}01$ near the centre of the α range. It should also be noted that F for $R = 1$ varies rather sharply near $\alpha = \pi/2$. We can expect, therefore, that at $R = 1$, the deformation may show a small jump (without exhibiting a noticeable amount of w_α) as α crosses $\pi/2$. This possibility seems feasible when we examine the stability of the static homogeneous deformation against time dependent perturbations (see § 4).

With this background it is relatively straightforward to appreciate the nature of variation of distortion when the magnetic polar angle α is held constant and the azimuthal angle β is varied. In this case **H** moves on the surface of a cone having an angle of 2α. Remembering that the ground state is homogeneously oriented, the following observations can be made.

From equations (3.1) and (3.2) the relevant range for β variation is $0 \leqq \beta \leqq \pi$ at a given α. In addition,

$$\beta \rightarrow \pi - \beta; \quad \phi \rightarrow -\phi; \quad \theta \rightarrow -\theta \tag{3.7}$$

is a symmetry operation for equation (2.6). Also, $\alpha = (\pi/2) \pm \alpha_1$ are equivalent if $\theta \rightarrow -\theta$. Hence it is sufficient to choose α values in the range $0 \leqq \alpha \leqq \pi/2$.

When $\alpha = 0$, **H** lies in the xy plane as β is varied and so does **n**. The deformation is pure twist and for $\beta = \pi/2$, we can define the twist Freedericksz threshold $H_2 = (\pi/2h)(K_2/\mu_o\chi_a)^{1/2}$; H_2 can be used for measuring H. When $\alpha \neq 0$, however, the distortion is splay–bend close to $\beta = 0$ or π; for intermediate values of β, the deformation is a combination of splay, twist and bend, with the twist component becoming important near the centre of the β range. For $\alpha \neq 0$ and $\beta = \pi/2$, we can define the characteristic field $H_0(\alpha)$ from equation (3.6) which is a function of α. For uniformity of description the splay Freedericksz threshold H_F is again used to form the reduced field.

Figure 3 shows the variations of θ_m and ϕ_m as functions of β for different values of α. Figures 2 (*c*) and (*d*) depict the corresponding variations of the total free energy F with β. The qualitative interpretation of these diagrams follows closely that presented for figure 1. For instance, $|\theta_m| < \alpha$ is the range of θ_m. When α is close to zero and the deformation practically confined to the xy plane (see figures 3 (*a*) and (*b*)) one finds type A behaviour for the low field and type B for high fields. As before, the bistability width

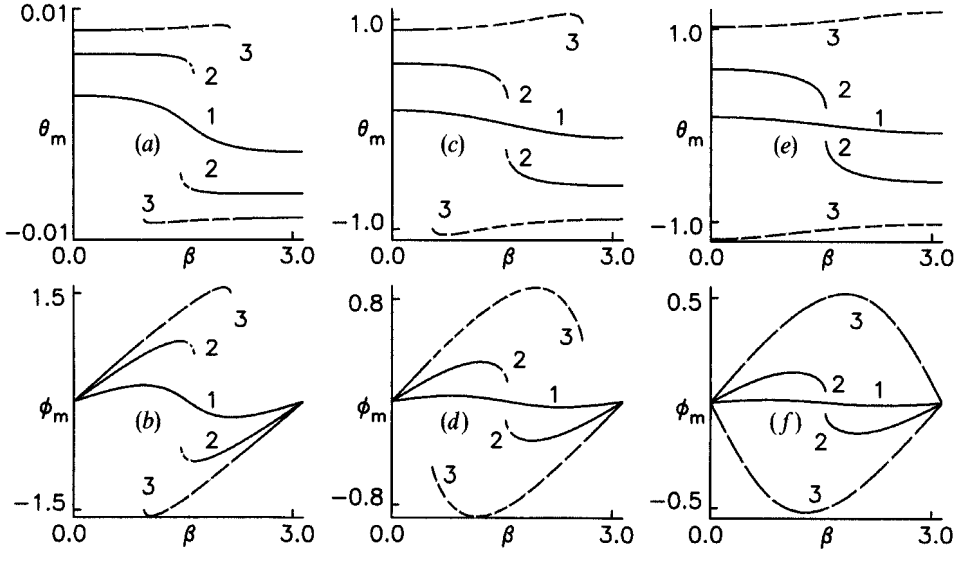

Figure 3. Plots of θ_m and ϕ_m versus β for different R and α. The ground state is homogeneous along the x axis and is rigidly anchored at the boundaries. $\alpha = (a)$, (b) 0·01 (c), (d) 1·17 (e), (f) 1·36 rad. Curves have been drawn for $R = (1)$ 0·5 (2) 1·0 (3) 1·5. Depending upon the values of α and R we get distortion variations of type A, B or C in contrast to the single angle description [11–14] where only type A or B is met (see § 3.1.).

w_β increases with R. When α is sufficiently high, **n** can escape out of the xy plane via a splay–bend distortion (see figures 3 (*c*) and (*d*)); w_β increases for the higher field ($R = 1{\cdot}5$) but diminishes for the lower one ($R = 1{\cdot}0$). At still higher α, we observe type C behaviour for $R = 1{\cdot}5$ and type A for the lower fields. There exists an intermediate range of R (results have not been shown) over which we find type B variation.

3.2. $\phi_\pm = \pm\phi_0$; $\theta_\pm = 0$

The ground state is twisted with total twist $= 2\phi_0$, without pretilt at the boundaries. Results for this case are presented briefly. If the material is a nematic then $k_2 = 0$ and $2\phi_0 < \pi/2$. The ground state is described by $\theta(z) = 0$ and an antisymmetric twist $\phi(z) = (\phi_0/h)z$. Because of this reason the deformation for general orientations of **H** will not be symmetric. When $\alpha = \pi/2$ (**H** is along z, hence β is not relevant) a symmetric $\theta(z)$ and an antisymmetric $\phi(z)$ can be expected when $H > H_T$ with [21]

$$H_T = [\{K_1(\pi^2/4h^2) + (K_3 - 2K_2)(\phi_0^2/h^2)\}/\mu_0\chi_a]^{1/2}. \tag{3.8}$$

When $\phi_0 \to 0$, $H_T \to H_F$. Hence it seems reasonable to employ H_T for defining R.

For $\beta = 0$ and arbitrary values of α we can expect a deformation with θ symmetric and ϕ antisymmetric. For general values of β, $\theta(z)$ and $\phi(z)$ will be asymmetric when α takes arbitrary values. On the basis of what has been discussed here it is possible to reach another conclusion. Suppose at a sufficiently elevated H, α is varied with $\beta \neq 0$. To start with, the deformation will be asymmetric. When α reaches $\pi/2$, $\theta(z)$ should become symmetric and $\phi(z)$ antisymmetric; when α is varied further, the distortion should again become asymmetric.

Depending upon **H** and ϕ_0, two types of asymmetric solutions are possible for $\phi(z)$. In the first kind, which we shall call $\mathscr{A}_\phi$, $\phi(z)$ varies monotonically from ϕ_- at $z = -h$ to ϕ_+ at $z = +h$. In the second type, referred to as $\mathscr{E}_\phi$, $\phi(z)$ becomes an extremum at some intermediate point $z_m : |z_m| < h$. As $\theta_\pm = 0$, $\theta(z)$ is always of the $\mathscr{E}_\theta$ type, viz. $\theta(z)$ always reaches an extremum at some point between the sample planes. It is found that $\phi(z)$ conforms to the $\mathscr{A}_\phi$ or the $\mathscr{E}_\phi$ type of variation over certain ranges of magnetic tilt depending upon the values of R and ϕ_0. It is therefore, found convenient to use $\phi_C = \phi(z = 0)$ and $\theta_C = \theta(z = 0)$ as measures of the deformations.

Plots of θ_C and ϕ_C as functions of α (for different β) and of β (for various α) can be drawn at given values of R and ϕ_0. At a given ϕ_0 the plots are found to be qualitatively similar to those of θ_m and ϕ_m of figures 1 and 3 and hence they have not been included. As in figures 1 and 3, the plots of θ_C and ϕ_C are symmetric with respect to the mid-point of the range of magnetic tilt (α or β) and this in spite of $\theta(z)$ and $\phi(z)$ being themselves generally asymmetric with respect to $z = 0$. The relevance of this observation will become clear in the next section.

The table summarizes quantitatively the different aspects of the variation of the distortion for three values of twist. Relatively high values of R have been chosen so that type B or type C variations are produced. Both α and β variations have been represented. The interpretation of the results is not straightforward, but the following points may be noted.

When α is sufficiently small, w_β decreases as ϕ_0 is enhanced; interestingly, this trend gets reversed when α is high enough ($= 1{\cdot}17$). For $\alpha = 1{\cdot}36$, $R = 1{\cdot}5$, $w_\beta = \pi$ for all three values of twist (type C behaviour).

The α variation at a given β does not show the same regularity as the β variation discussed previously. It is found, however, that w_α generally increases with β for a given ground state twist. It also appears that w_α decreases in general with increasing ϕ_0.

Type B variation of deformation is considered except (†) which indicates type C behaviour. α and β are, respectively, the magnetic polar and azimuthal angles. $2\phi_0$ is the ground state twist. All angles are expressed in radian. Material constants as in equation (2.9). $R = H/H_T$ is the reduced field where H_T is the Freedericksz threshold from equation (3.8).

I. *Bistability width w_α for α variation*
$R = 1{\cdot}75$. Different values of β and ϕ_0 have been chosen.

ϕ_0	$\beta \to 0{\cdot}01$	0·19	0·39	0·78
0·00	1·04	1·08	1·20	π(†)
0·39	0·64	0·70	1·30	1·90
0·78	0·31	0·36	0·41	0·74

II. *Bistability width w_β for β variation*
$R = 1{\cdot}5$. Different values of α and ϕ_0 have been chosen.

ϕ_0	$\alpha \to 0{\cdot}01$	0·39	0·78	1·17
0·00	1·18	1·19	1·28	2·03
0·39	0·94	0·98	1·18	2·22
0·78	0·46	0·54	0·90	2·80

III. *Effect of variation of elastic constant on bistability width*
$\phi_0 = 0{\cdot}39$. $R = 1{\cdot}5$. At a time the values of two elastic constants are held fixed as in equation (2.9) and the value of the third (in units of 10^{-12} N) is changed as shown.

	$\beta = \pi/4$	$\alpha = \pi/4$
$K_1 = 0{\cdot}925$	$w_\alpha = 0{\cdot}58$	$w_\beta = 0{\cdot}42$
$= 1{\cdot}850$	$= 1{\cdot}06$	$= 1{\cdot}18$
$= 3{\cdot}700$	$= \pi$(†)	$= 2{\cdot}39$
$K_2 = 0{\cdot}65$	$= \pi$(†)	$= 2{\cdot}00$
$= 1{\cdot}30$	$= 1{\cdot}06$	$= 1{\cdot}18$
$= 2{\cdot}60$	$= 0{\cdot}84$	$= 0{\cdot}54$
$K_3 = 1{\cdot}01$	$= 1{\cdot}63$	$= 1{\cdot}66$
$= 2{\cdot}02$	$= 1{\cdot}06$	$= 1{\cdot}18$
$= 4{\cdot}04$	$= 0{\cdot}68$	$= 0{\cdot}98$

These studies can be extended to long pitch cholesterics (pitch ~ sample thickness). While it is rather difficult to give a detailed description in the present limited format, it may not be out of place to indicate certain interesting ramifications that can be expected. It is convenient to assume that the director is rigidly anchored at the two boundaries such that the ground state retains the equilibrium pitch (P_0). It is then natural to employ the threshold [21]which can be defined when **H** is directed along the z axis:

$$H_C = [\{(\pi^2/4)K_1 + K_3\phi_0^2\}/\mu_0\chi_a h^2]^{1/2}.$$

The reduced field $R = H/H_C$. For $H > H_C$ we expect, as before, a distortion with $\theta(z)$ symmetric and $\phi(z)$ antisymmetric. The expression for H_C is meaningful only when P_0 is

large enough compared to the sample thickness or, equivalently, when ϕ_0 is sufficiently small. When ϕ_0 exceeds a critical value $\phi_0 = (\pi/2)\,[K_2K_3/(K_3-K_2)(K_3+2K_2)]^{1/2}$, the homogeneous deformation may not occur at $\alpha = \pi/2$ because of being energetically infeasible (see § 5). For the material parameters from equation (2.9), $\phi_0 = 1{\cdot}37$ rad. It should be interesting to compare the variation of distortion with magnetic tilt for $\phi_0 < \phi_0$ and for $\phi_0 > \phi_0$.

3.3. $\phi_\pm = 0$; $\theta_\pm = \theta_1$

The ground state with $0 < \theta_1 < \pi/2$ is uniformly tilted with respect to the x axis in the xz plane without any twist superposed on it. In this case, as in section 3.1, both $\theta(z)$ and $\phi(z)$ are symmetric relative to the sample centre. For the variation of α, at a given β, we can choose the range $\theta_1 \leqq \alpha \leqq \theta_1 + \pi$; it is convenient to vary β over the range $0 \leqq \beta \leqq \pi$ for the given α. H is measured in terms of H_F. Some of the symmetries discussed in section 3.1 may no longer be valid.

Suppose $\beta = 0$ and α, the magnetic polar angle, is varied at a given R. The distortion is of the splay–bend kind and there is no twist. A simple calculation shows that the total free energy F varies in a symmetric way with respect to $\alpha = \theta_1 + \pi/2$, the mid-point of the range, i.e. $F(\alpha = \theta_1 + \alpha_1) \approx F(\alpha = \theta_1 + \pi - \alpha_1)$. However, the deformations for the two values of α are somewhat different. It can be seen (see, for instance, figure 1 of [14]) that $\theta_m\ (\alpha = \theta_1 + \alpha_1) - \theta_1 \approx \theta_1 - \theta_m(\alpha = \theta_1 + \pi - \alpha_1)$. This essentially means that when α is increased from $\alpha = \theta_1$, θ_m increases above θ_1; when α is diminished from $\alpha = \pi + \theta_1$, θ_m decreases below θ_1. In the two cases the distribution of splay and bend in the deformation is different, but both states will have almost the same free energy provided that α has been varied by the same amount from the two edges of its range. It will now be clear that in case **H** is swung out of the xz plane by some angle β, the effect on the distortion at the two values of α will be quite different as the splay–bend will couple with twist in completely different ways. Hence, when $\beta \neq 0$, the deformations $\theta(z)$, $\phi(z)$ at $\alpha = \theta_1 + \alpha_1$ and $\alpha = \pi + \theta_1 - \alpha_1$ will be quite different; at these two values of α, even the total free energies should be different. This difference, which is negligible for $\beta = 0$, can be expected to increase when β is enhanced and become maximum when $\beta = \pi/2$. Simply put, we can think of asymmetry in the nature of change of distortion when the magnetic tilt is varied along opposite directions from the two ends of its range—a situation completely absent when the ground state is homogeneously aligned.

Figure 4 depicts plots of θ_m and ϕ_m as functions of α for different β at three R values. A relatively low pretilt of $\theta_1 = 0{\cdot}19$ rad has been used. Asymmetry is evident and becomes more pronounced as β assumes higher values. This becomes especially clear from the F versus α curves (see figure 2(*e*)) drawn for a higher pretilt ($\theta_1 = 0{\cdot}78$).

The plots of θ_m and ϕ_m versus β for different α are shown in figure 5 for a pretilt of $\theta_1 = 0{\cdot}39$ rad. When the magnetic polar angle α is small, the deformation varies in a symmetric way for equal variations of β from either end of its range. When α is sufficiently high, there again occurs a marked asymmetry like the kind presented in figure 4; a representative diagram of F versus β (see figure 2(*f*)) completes the description.

The combined effects of director pretilt at the boundaries and an imposed twist in the ground state may be interesting. In this case it may be possible to consider ground state twists higher than $\pi/2$ [25]. The ground state twist should make the deformation asymmetric with respect to the sample centre. The director pretilt at the boundaries should make asymmetric even the nature of change of distortion for magnetic tilt variations from either end of the range. A detailed discussion is postponed to the future.

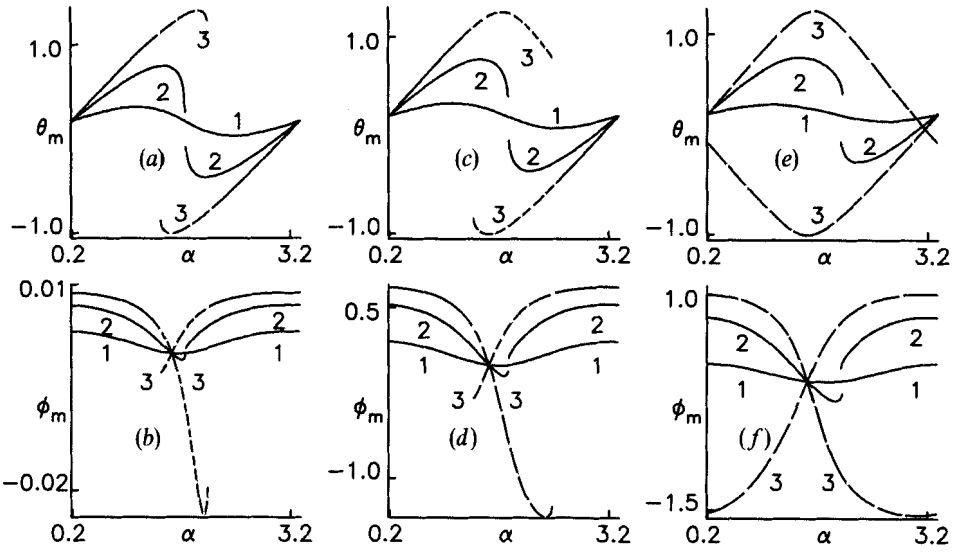

Figure 4. Variations of θ_m and ϕ_m as functions of α. The ground state is uniformly oriented in the xz plane making angle $\theta_1 = 0{\cdot}19$ with the x axis. The reduced field R has the same definition as before. Curves are drawn for $R = (1)\,0{\cdot}5\,(2)\,1{\cdot}0\,(3)\,1{\cdot}5$. $\beta = (a), (b)\,0{\cdot}01\,(c), (d)\,0{\cdot}78\,(e), (f)\,1{\cdot}17$ rad. The distortion changes by different amounts when α is increased from θ_1 or decreased from $\pi + \theta_1$ at given R and β. This may be due to the different kinds of couplings between the splay–bend and twist components in the two cases (see § 3.3); see also figures 5 and 2(*e*).

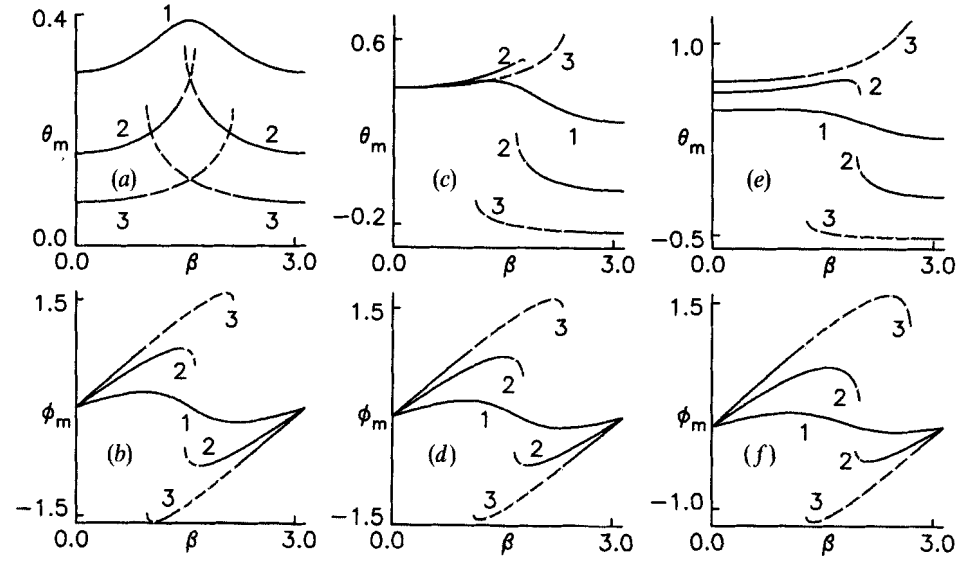

Figure 5. Plots of θ_m, ϕ_m versus β at different values of R and α. The ground state is uniformly tilted in the xz plane making an angle $\theta_1 = 0{\cdot}39$ with the x axis. Curves are drawn for $R = (1)$ 0·5 (2) 1·0 (3) 1·5. $\alpha = (a)$, (*b*) 0·0 (*c*), (*d*) 0·39 (*e*), (*f*) 0·78. The distortion changes symmetrically with respect to the centre of the β range for $\alpha = 0$. When α is different from zero, an asymmetry can be detected (see § 3.3); see also figures 4 and 2(*f*).

3.4. *Nematic with* $\chi_a < 0$

To study this case the elastic constant values of equation (2.9) are used but the sign of χ_a is reversed. It is well-known that when **H** is imposed on a $\chi_a < 0$ nematic, **n** tends to align normal to **H**. Under the joint actions of surface anchoring and **H** it is possible to consider homogeneous deformations in this case also. Certain intricacies can, however, arise and to understand these it is necessary to appreciate how the distortion changes with magnetic tilt. Unless otherwise stated a homogeneous ground state is assumed ($\theta_\pm = \theta = 0$).

For a $\chi_a < 0$ nematic, the only Freedericksz direction is with **H** along the uniform **n**. For homogeneous alignment the twist Freedericksz threshold $H_2'' = (\pi/2h) \times (K_2/\mu_o|\chi_a|)^{1/2}$ is lower than the splay Freedericksz threshold $H_F'' = (\pi/2h)(K_1/\mu_o|\chi_a|)^{1/2}$ as $K_2 < K_1$. The deformation for general magnetic tilt can become a combination of splay, twist and bend; hence for uniformity we shall use H_F'' to measure H.

Figure 6 contains the plots of θ_m and ϕ_m versus the magnetic azimuthal angle β for various values of α and reduced field $R = H/H_F''$. As $\beta = \pm\pi/2$ correspond to positions of vanishing magnetic torque on **n**,it is natural to vary β in the range $-\pi/2 \leqq \beta \leqq \pi/2$. Comparison of figure 6 with figure 3 (for a $\chi_a > 0$ nematic) shows that the ϕ_m curves are similar but the θ_m curves are not. Interestingly, the θ_m curves of figure 6 are similar to the ϕ_m curves of figure 1 (α variation: $\chi_a > 0$ case). When α is sufficiently small and R high enough we find type B variation (see figures 6 (*a*)–(*d*)). When α is increased (see figures 6 (*e*) and (*f*)) we again find only type A behaviour—continuous variation of deformation but no bistability—for the same high field. As α is raised to still higher values the curves only get more rounded (these have not been presented).

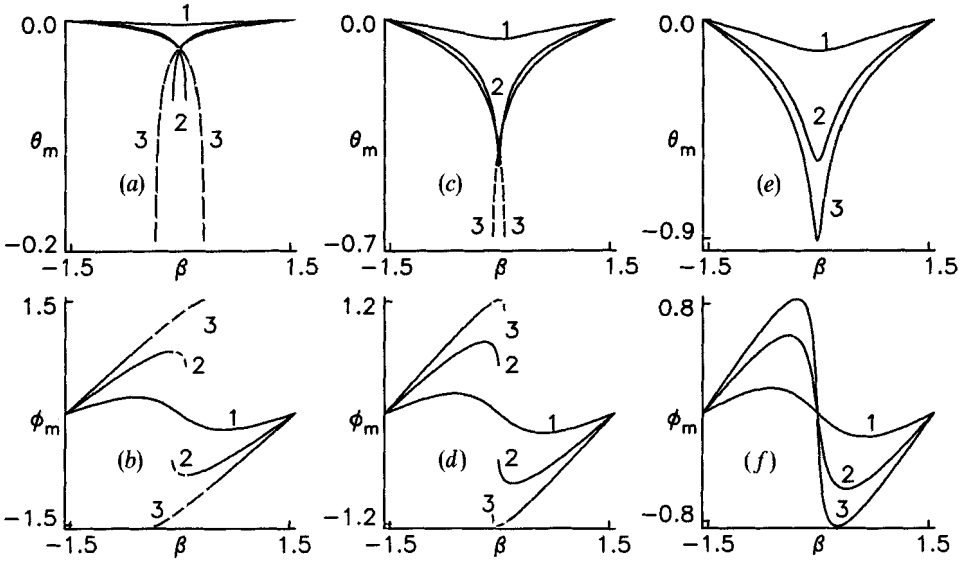

Figure 6. Nematic with $\chi_a < 0$. Variations of θ_m, ϕ_m with β for different values of α and reduced field $R = H/H_F''$ where H_F'' is the splay Freedericksz threshold. Ground state is homogeneous along x. Material parameters are as in equation (2.9) except that the sign of χ_a is reversed. $R = (1)\ 0{\cdot}5\ (2)\ 1{\cdot}0\ (3)\ 1{\cdot}5$. $\alpha = (a), (b)\ 0{\cdot}01\ (c), (d)\ 0{\cdot}15\ (e), (f)\ 0{\cdot}39$. Comparison with figure 1 ($\chi_a > 0$ case) shows that while the ϕ_m curves are similar, the θ_m curves are not. Only deformation variations of types A and B can be seen as increase in α causes a change over from type B to type A variation at a given R (see § 3.4).

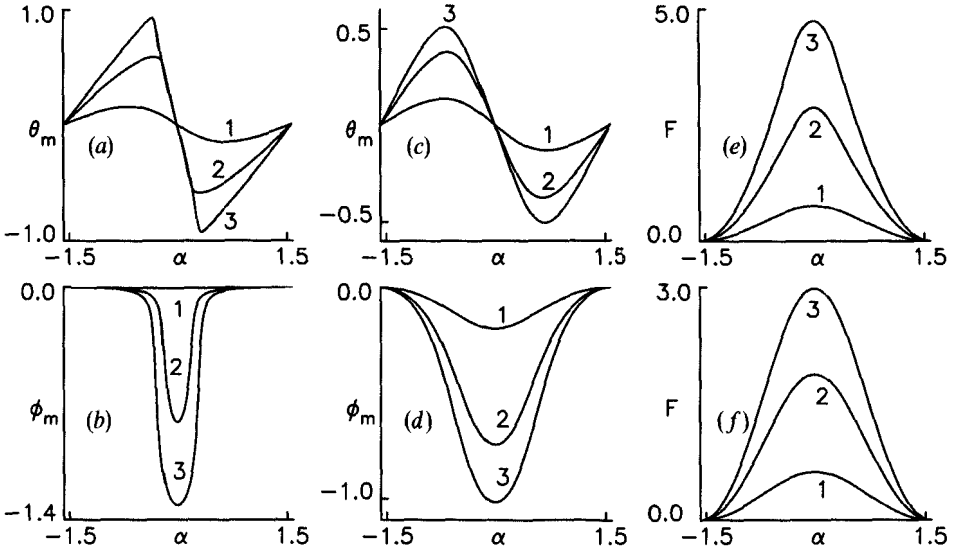

Figure 7. Nematic with $\chi_a < 0$. Plots of θ_m, ϕ_m and F versus α. Ground state is homogeneous along x. R is defined as in figure 6. $R = (1)\,0{\cdot}5\,(2)\,1{\cdot}0\,(3)\,1{\cdot}5$. $\beta = (a), (b), (e)\,0{\cdot}01\,(c), (d), (f)\,0{\cdot}39$. The deformation change conforms to type A only. When β is small, (*a*), (*b*) a sharp change can be discerned in θ_m as α crosses a certain value α_C for sufficiently high R. This is accompanied by a steep build up of the twist component. When $\beta = 0$, α_C actually corresponds to a threshold change over from splay–bend deformation to a splay–bend–twist distortion (see § 3.4; see also figure 8). (*e*) shows that F varies continuously with α even when β is small. Interestingly, F for the present case is positive (compare with the sign of F in figure 2 for $\chi_a > 0$ nematic).

Figure 7 shows the variations of θ_m, ϕ_m and F as functions of the magnetic polar angle α for different values of β and R. As $\alpha = \pm\pi/2$ are positions of zero magnetic torque on **n**, we select the range $-\pi/2 \leqq \alpha \leqq \pi/2$. For $\beta = 0{\cdot}39$ (see figures 7 (*c*) and (*d*)) there are no discontinuous changes in the deformation even at a sufficiently elevated field ($R = 1{\cdot}5$); curves for still higher β are found to be similar in shape to those of figures 7 (*c*) and (*d*) except that the extrema of $\theta_m(\alpha)$ and $\phi_m(\alpha)$ get scaled down. For $\beta = 0{\cdot}01$, however, the results are more interesting. It is found that when α crosses a critical value $|\alpha_C| (< \pi/2)$, θ_m changes somewhat sharply when R is high enough. Figure 7 (*b*) shows that at the same point, ϕ_m increases sharply from a value close to zero (when R is low, ϕ_m remains zero for all α). This has all the trappings of a threshold phenomenon, but the F versus α curve (see figure 7 (*e*)) does not show perceptible discontinuity at $\alpha = |\alpha_C|$ (it is instructive to compare the sign of F here with that of F for $\chi_a > 0$, (see figure 2). Thus the twist appears to grow continuously at this point.

3.4.1. *Twist instability of splay–bend distortion*

To understand this qualitatively, let us consider what happens when $\beta = 0$ so that a variation of α rotates **H** in the xz plane. When $\alpha = 0$, **H** is along the Freedericksz direction; if $H > H_2''$, a pure twist deformation $\phi(z)$ will come into existence with **n** lying in the xy plane. Suppose, instead, we had started with $\alpha = \pi/2$ (**H** along z),then **H** would exert no torque on **n**, regardless of H. If α is varied slightly, a splay–bend distortion can occur due to the increase in the magnetic torque. As the deformation and field are both in the xz plane we can expect the θ distortion to get enhanced as α is varied further away

from the z axis. For a $\chi_a<0$ nematic, **H** tends to push **n** towards a plane normal to **H**. The stable deformation for $\alpha=0$ (when **H** is along the x axis) is a pure twist. Hence, once **H** is sufficiently tilted towards the **x** axis it is possible that **H** might couple with twist perturbations to cause **n** to twist out of the xz plane. An identical argument can be given when we start with $\alpha=-\pi/2$ and rotate **H** towards the x axis.

When $\beta=0$ and $\phi(z)$ develops at $\alpha=\alpha_C$, both parities of twist can grow (i.e. twists with $\phi_m>0$ and $\phi_m<0$; this becomes clear presently when we present a linear stability analysis) as both states will have the same free energy. It is quite possible, therefore, that when $\beta=0$ and α crosses α_C, the distortion in the sample will break up into domains separated by domain walls; sufficiently far away from a wall the distortion will be homogeneous (θ, ϕ being functions of z alone) with ϕ having a certain parity (i.e. $\phi_m>0$ on one side of the wall and $\phi_m<0$ on the other side). This degeneracy has been lifted in figure 7 (*b*) by making β slightly different from zero. It should be clear that if β were $-0{\cdot}01$, the ϕ_m curve would be above the α axis.

A linear perturbation analysis is employed. The initial static deformation is specified by

$$\mathbf{n}=(C_\theta, 0, S_\theta); \quad \theta=\theta(z); \quad \mathbf{H}=(HC_\alpha, 0, HS_\alpha); \tag{3.9}$$

$$\left.\begin{aligned} f_2(\theta)\theta_{,zz}+[(df_2/d\theta)\theta_{,z}^2+\mu_o\chi_a H^2\sin(2\alpha-2\theta)]/2=0; \\ \theta(z=\pm h)=\theta_\pm. \end{aligned}\right\} \tag{3.10}$$

Perturbations are now imposed such that **n** becomes

$$\mathbf{n}''=[\cos(\theta+\theta'')\cos\phi'', \sin\phi'', \sin(\theta+\theta'')\cos\phi'']. \tag{3.11}$$

The total free energy density F'' is written down retaining terms up to the second order in θ'', ϕ'' and their derivatives. When F'' is extremized with respect to the perturbations using equation (3.10) we obtain the following pair of torque equations and boundary conditions:

$$\begin{aligned} &f_2(\theta)\theta''_{,zz}+(df_2/d\theta)\theta_{,z}\theta''_{,z}+\theta''[\theta_{,zz}(df_2/d\theta)-\mu_o\chi_a H^2\cos(2\alpha-2\theta) \\ &\quad+\tfrac{1}{2}(d^2f_2/d\theta^2)\theta_{,z}^2]=0; \quad \theta''(z=\pm h)=0, \end{aligned} \tag{3.12}$$

$$\left.\begin{aligned} &f_5(\theta)\phi''_{,zz}+(df_5/d\theta)\theta_{,z}\phi''_{,z}+\phi''[f_6(\theta)\theta_{,zz} \\ &\quad+f_7(\theta)\theta_{,z}^2-\mu_o\chi_a H^2\cos^2(\alpha-\theta)]=0; \quad \phi''(z=\pm h)=0; \\ &f_5(\theta)=K_2C_\theta^2+K_3S_\theta^2; \quad f_6(\theta)=(K_2-K_1)S_\theta C_\theta; \\ &f_7(\theta)=K_1S_\theta^2+K_2C_\theta^2+2(K_3-K_2)S_\theta^2. \end{aligned}\right\} \tag{3.13}$$

As ϕ'' is associated with the much weaker elastic constant K_2, it is clear that the uncoupled θ'' mode can be ignored while considering the linear threshold [26].

The method of solution is as follows. Starting with a value close to $\pi/2$, α is varied towards zero; for each value of α, $\theta(z)$ is determined from equation (3.10) and the compatibility condition evaluated from equation (3.13). The condition is found to be satisfied at a certain α_C which can be studied as a function of $R=H/H_F''$ for given $\theta_\pm$ or as a function of $\theta_\pm$ at a fixed R.

Figure 8 (*a*) depicts the variation of α_C with R for the homogeneous ground state; different material parameters have been used. For a given material, α_C decreases as R is diminished ; $\alpha_C\to0$ as $R\to H_2''/H_F''$ the twist Freedericksz threshold. At a given R, α_C increases when K_1 or K_3 is enhanced; **H** has to be rotated by a smaller angle away from

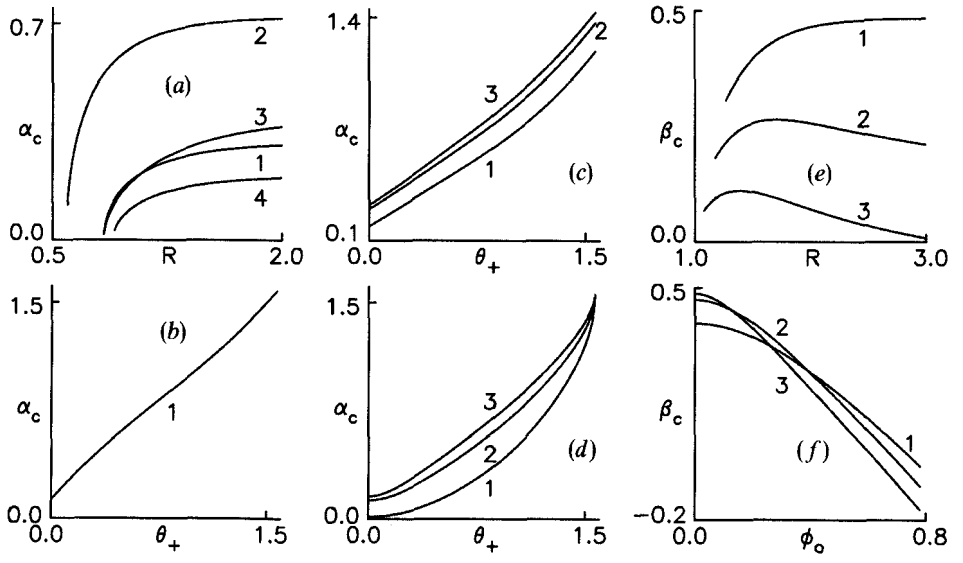

Figure 8. Plots of magnetic tilt thresholds as functions of different parameters. Nematic with $\chi_a < 0$. R is defined as in figure 6. A time independent linear perturbation analysis is used. (*a*)–(*d*) variation of α_C with R and boundary tilt of the director. The initial distortion is splay–bend from equations (3.9) and (3.10). α_C is the critical value of α such that when α, varied from $\pi/2$, crosses α_C, a twist can develop over and above the splay–bend deformation. Material parameters are as in figures 6 and 7 for (*b*), (*c*), (*d*). (*a*) α_C versus R for different material constants. The ground state is homogeneously aligned along x. The material constants are (in units of 10^{-12} N); $(K_1, K_2, K_3) = (1)$ as in equation (2.9), (2) (3·7, 1·3, 2·02), (3) (1·85, 1·3, 1·04), (4), (1·85, 1·5, 2·02). When $H \to H_2''$, the twist Freedericksz threshold, $\alpha_C \to 0$. (*b*) α_C versus θ_1 which is the uniform tilt of the ground state in the xz plane at $R = 1{\cdot}5$; curves for $R = 1{\cdot}0$, 2·0 lie close to this one and hence they have not been shown. (*c*) α_C versus θ_+ for $\theta_- = 0$; asymmetric anchoring of the director at the boundaries which means that the ground state has splay–bend deformation. $R = (1)$ 1·0 (2) 1·5 (3) 2·0. (*d*) α_C versus θ_+ for $\theta_- = -\theta_+$. Reversely pretilted case. The ground state is distorted. R values as in (*c*). Curves for $\theta_+ > \pi/4$ may be of only academic interest [27] (see § 3.4.1). (*e*) and (*f*) the ground state is a twisted nematic with twist $= 2\phi_0$. **H** is rotated in the xy plane. β_C is the threshold tilt at which the initial twist deformation becomes unstable against splay–bend fluctuations. (*e*) β_C versus R for $\phi_0 = (1)$ 0·0 (2) 0·39 (3) 0·6. (*f*) β_C versus ϕ_0 for $R = (1)$ 1·5 (2) 2·0 (3) 3·0 (see §3.4.2).

the z axis before a twist distortion starts to grow. This may be due to the increased elastic destabilizing torques associated with ϕ'' from equation (3.13). On the other hand, α_C diminishes when K_2 is increased at fixed R. Clearly, due to the increased elastic resistance from the twist elastic constant, **H** has to be moved closer to the x axis before a twist can develop.

Variation of α_C with the director boundary tilt can be studied at a fixed R. Increase in the uniform pretilt angle of the ground state $\theta_\pm = \theta_1$ (away from the homogeneous) causes α_C also to be augmented (see figure 8 (*b*)). When the pretilts at the boundaries are unequal ($\theta_- = 0$; θ_+ is varied; see figure 8(*c*)) α_C increases with θ_+. In this case the ground state is asymmetrically deformed. A similar variation is seen (see figure 8 (*d*)) for the reversely pretilted case with $\theta_- = -\theta_+$. The curves of figure 8 (*d*) may be of only theoretical significance for $\theta_+ > \pi/4$ as the antisymmetrically distorted ground state may not be stable [27].

3.4.2. *Splay–bend instability of twist deformation*

In an exactly analogous way we can investigate the situation in which **n** and **H** are initially confined to the xy plane so that the static distortion is given by

$$\mathbf{n}=(C_\phi, S_\phi, 0);\quad \phi=\phi(z);\quad \mathbf{H}=(HC_\beta, HS_\beta, 0);$$
$$K_2\phi_{,zz}+\tfrac{1}{2}\mu_o\chi_a H^2\sin(2\beta-2\phi)=0;\quad \phi(z=\pm h)=\phi_\pm. \tag{3.14}$$

Under static fluctuations θ'', ϕ'', **n** becomes

$$\mathbf{n}''=[\cos\theta''\cos(\phi+\phi''), \cos\theta''\sin(\phi+\phi''), \sin\theta'']. \tag{3.15}$$

The decoupled linearized equation [26] along with the relevant boundary conditions are

$$K_2\phi''_{,zz}-\mu_o\chi_a H^2\cos(2\beta-2\phi)\phi''=0;\quad \phi''(z=\pm h)=0; \tag{3.16}$$

$$\left.\begin{aligned} K_1\theta''_{,zz}+\theta''[2k_2\phi_{,z}+(2K_2-K_3)\phi^2_{,z}-\mu_o\chi_a H^2\cos^2(\beta-\phi)]=0;\\ \theta''(z=\pm h)=0;\end{aligned}\right\} \tag{3.17}$$

(for nematics we shall put $k_2=0$). When H is sufficiently high and β is varied from $\pm\pi/2$, the ϕ'' mode will form at the edges of the bistable region ($\beta=\pm\beta_o$, say). It is , however, likely that the θ'' mode might grow at $\beta=\pm\beta_C$, before β reaches $\pm\beta_o$:$|\beta_o|<|\beta_C|<\pi/2$. If this happens we can say that the static twist deformation $\phi(z)$ undergoes an out of the plane instability due to the splay–bend perturbation θ''. The threshold azimuthal angle β_C, calculated from equation (3.17), varies with reduced field R and ground state twist as shown in figures 8 (*e*) and (*f*). It will be seen that every β_C versus R curve terminates (see figure 8 (*e*)) at a certain R value; this is where β_C crosses beyond the bistable region: $\beta_C<\beta_o$.

Unlike figures 7 (*a*) and (*b*) which contain threshold-like behaviour, figures 6 (*a*) and (*b*) (for $\alpha=0{\cdot}01$) do not appear to indicate the existence of the θ'' threshold. One reason is that θ'' is associated with the splay and bend elastic constants which are both higher than the twist constant; because of this reason θ'' cannot develop sharply over the twist. The other reason is that this α value is not small enough. If we fix α even lower ($=0{\cdot}005$) the θ_m, ϕ_m verses β curves for $R=1$ and $1{\cdot}5$ show sharper variations as β crosses β_C (these diagrams have not been included).

3.5. *Scaling analysis; effect of varying elastic constants*

It is assumed that $\chi_a>0$ for the rest of the discussion. The sample thickness is one of the parameters which enters the picture. So far we have obtained all results for a given sample thickness. A question does often arise as to how results get affected when the sample thickness is changed [3]. In particular we want to find out how change in sample thickness can affect bistability width (w_α or w_β) when we have a type B variation of distortion.

This is easily achieved by changing the variable from z to $\xi=z/h$ in equation (2.6). It is then found that h explicitly occurs only with H^2 in terms whose coefficients are proportional to $\chi_a h^2H^2$ (we remember that the material is a nematic; for a cholesteric there occurs an additional term whose coefficient is k_2h). It is clear that for a nematic the solutions of equations (2.6) and (2.8) will remain unaltered if the product (Hh) remains unchanged when h is varied, i.e. if $h\to h\sigma$, $H\to H/\sigma$, where σ is a constant. Noting the

definition of the splay Freedericksz threshold ($H_F \sim h^{-1}$) it is clear that for given material and boundary conditions from equation (2.8) the solutions of equation (2.6) will remain unaltered for the same reduced field $R = H/H_F$ for any sample thickness. Hence, all attributes of the solution such as the bistability width will also remain unchanged at fixed R provided that the anchoring is rigid. It must be borne in mind that changes in h will cause scaled changes in the total free energy of the sample provided that the lateral dimensions of the sample are kept fixed; i.e., if $h \to h\sigma$, then, $F \to F/\sigma$. Thus the curves of F versus magnetic tilt retain their shape, only the value of F will change. To give a specific example, let $\beta = 0{\cdot}01$. Then for a sample thickness of 20 μm the plots of θ_m and ϕ_m versus α will be the same as the curves of figures 1 (*a*) and (*b*) for the three R values; the corresponding plots of F versus α will also be identical to those of figure 2 (*a*) except that the F axis scale has to be multiplied by a factor of ten. These conclusions are qualitatively identical to those arrived at for the single angle description [14]: needless to say, an experimental check is possible. It must be remembered that the above scaling is specific to rigid anchoring at the boundaries; scaling will not hold for weak anchoring; scaling will also fail for a cholesteric.

Changes in the values of the different elastic constants can affect the nature of the solution, especially the bistability width. In principle this should be done for various kinds of boundary conditions. For simplicity, however, a twisted nematic with $\phi_0 = 0{\cdot}39$ is chosen. The elastic constant values are shown in the table. H is assumed to be sufficiently high ($R = 1{\cdot}5$) so that bistability results in all cases. At given β ($= \pi/4$), w_α is found to increase with K_1; w_α diminishes when K_2 or K_3 is enhanced. A similar trend is found when α is held constant and w_β is studied for different sets of elastic constants.

4. Dynamics, generalizations and stability analysis

4.1. *Governing equations for finite deformations*

So far the magnetic tilt has been assumed to change in small steps and consequently dissipative effects have been ignored. In a real situation transient effects should occur every time **n** changes due to the variation of magnetic tilt; in particular, when the magnetic tilt overshoots the edge of the bistable region the deformation change to a lower energy state will be accompanied by transient flow. In such a situation it is necessary to assume that

$$\mathbf{n} = (C_\Theta C_\Phi,\ C_\Theta S_\Phi,\ S_\Theta); \quad \Theta = \Theta(z, t); \quad \Phi = \Phi(z, t). \tag{4.1}$$

In this case, Θ, Φ can give rise to viscous stresses σ_{zx}, σ_{zy} which, in turn, bring into existence a velocity field

$$\mathbf{v} = [v_x(z, t),\ v_y(z, t), 0]. \tag{4.2}$$

Incompressibility and the no-slip condition at the boundaries require that **v** cannot have a z component. In the most general case we get four coupled equations

$$\left.\begin{aligned} &f_2(\Theta)\Theta_{,zz} + [(df_2/d\Theta)\Theta_{,z}^2 - (df_3/d\Theta)\Phi_{,z}^2]/2 - (\partial f_4/\partial\Theta) \\ &\quad - (df_1/d\Theta)\Phi_{,z} - \gamma_1\dot{\Theta} - g_3(\Theta, \Phi)v_{x,z} - g_6(\Theta, \Phi)v_{y,z} = 0; \\ &f_3(\Theta)\Phi_{,zz} + (df_1/d\Theta)\Theta_{,z} + (df_3/d\Theta)\Theta_{,z}\Phi_{,z} - (\partial f_4/\partial\Phi) \\ &\quad - \gamma_1 C_\Phi^2\dot{\Phi} + g_4(\Theta, \Phi)v_{x,z} - g_7(\Theta, \Phi)v_{y,z} = 0, \end{aligned}\right\} \tag{4.3}$$

$$
\left.\begin{aligned}
&\sigma_{zx,z}-\rho\dot{v}_x=0;\quad \sigma_{zy,z}-\rho\dot{v}_y=0;\\
&\sigma_{zx}=g_1(\Theta,\Phi)v_{x,z}+g_2(\Theta,\Phi)v_{y,z}+g_3(\Theta,\Phi)\dot{\Theta}+g_4(\Theta,\Phi)\dot{\Phi};\\
&\sigma_{zy}=g_2(\Theta,\Phi)v_{x,z}+g_5(\Theta,\Phi)v_{y,z}+g_6(\Theta,\Phi)\dot{\Theta}+g_7(\Theta,\Phi)\dot{\Phi};\\
&g_1=\mu_1 S_\Theta^2 C_\Theta^2 C_\Phi^2+[\mu_4+(\mu_5-\mu_2)S_\Theta^2+(\mu_3+\mu_6)C_\Theta^2 C_\Phi^2]/2;\\
&g_2=C_\Theta^2 S_\Phi C_\Phi[\mu_1 S_\Theta^2+(\mu_3+\mu_6)/2];\quad g_3=(\mu_3 C_\Theta^2-\mu_2 S_\Theta^2)C_\Phi;\\
&g_4=-\mu_2 S_\Theta C_\Theta S_\Phi;\quad g_5=g_1(\Theta,\Phi+\pi/2);\\
&g_6=-g_3(\Theta,\Phi+\pi/2);\quad g_7=-g_4(\Theta,\Phi+\pi/2);
\end{aligned}\right\}\tag{4.4}
$$

a superposed dot denotes the time derivative; a subscripted comma denotes a partial derivative; σ_{zx}, σ_{zy} are components of the viscous stress tensor; ρ is the density; the μ_i are the viscosity coefficients of the nematic ; $\gamma_1=\mu_3-\mu_2$ is the twist viscosity coefficient. The third component of the force equation which relates the z derivative of the hydrostatic pressure to elastic and viscous effects has been left out as it does not enter the picture. It is usual to ignore the inertial terms (proportional to ρ) as they are generally unimportant for thin samples. The boundary conditions for **n** and **v** become

$$
\Theta(z=\pm h,t)=\Theta_\pm;\quad \Phi(z=\pm h,t)=\Phi_\pm;\quad v_x(z=\pm h,t)=0;v_y(z=\pm h,t)=0.\tag{4.5}
$$

Let us first consider a nematic ($k_2=0$). The same procedure adopted in [14] can also be used here to put equations (4.3) and (4.4) into dimensionless form. To do this, equations (4.3) are divided by K_1. Now variables $\xi=z/h$, $u=t/\tau$ are employed where $\tau=\gamma_1 h^2/K_1$ is a characteristic time. The functions $J_i=f_i/K_1$ ($i=2,3,4$) become dimensionless as they depend only on elastic ratios. The H terms in equation (4.3) can be written in terms of R. By defining the dimensionless viscous functions $G_i=g_i/\gamma_1$ ($i=1$ to 7), and dimensionless velocities $V_x=v_x\tau/h$, $V_y=v_y\tau/h$, equations (4.3) and (4.4) can be rewritten as

$$
\left.\begin{aligned}
&J_2(\Theta)\Theta_{,\xi\xi}+[(dJ_2/d\Theta)\Theta_{,\xi}^2-(dJ_3/d\Theta)\Phi_{,\xi}^2]/2-(\partial J_4/\partial\Theta)\\
&\quad-\Theta_{,u}-G_3(\Theta,\Phi)V_{x,\xi}-G_6(\Theta,\Phi)V_{y,\xi}=0;\\
&J_3(\Theta)\Phi_{,\xi\xi}+(dJ_3/d\Theta)\Theta_{,\xi}\Phi_{,\xi}-(\partial J_4/\partial\Phi)-\Phi_{,u}\\
&\quad+G_4(\Theta,\Phi)V_{x,\xi}-G_7(\Theta,\Phi)V_{y,\xi}=0;\\
&[G_1(\Theta,\Phi)V_{x,\xi}+G_2(\Theta,\Phi)V_{y,\xi}+G_3(\Theta,\Phi)\Theta_{,u}+G_4(\Theta,\Phi)\Phi_{,u}]_{,\xi}=0;\\
&[G_2(\Theta,\Phi)V_{x,\xi}+G_5(\Theta,\Phi)V_{y,\xi}+G_6(\Theta,\Phi)\Theta_{,u}+G_7(\Theta,\Phi)\Phi_{,u}]_{,\xi}=0.
\end{aligned}\right\}\tag{4.6}
$$

It can be seen that for given material and boundary conditions, the only free parameter is R. If R is also fixed, equation (4.6) will yield solutions $\Theta(\xi,u)$ and $\Phi(\xi,u)$ which will be independent of sample thickness. It must be noted that τ depends on h.

Keeping in mind the results of scaling of the static equations (see section 3.5) the following conclusions can be reached. Suppose we perform a static experiment on two

sample thicknesses ($2h_1, 2h_2$) with the same high reduced field in both cases. We should get identical θ_m, ϕ_m curves (i.e. same bistability width w_α or w_β) in both cases. If we study the transition times near the edge of the bistability region we should get different results for the two cases. If T_1, T_2 are the transition times for the two samples the definition of τ indicates that $(T_1/T_2) \propto (h_1/h_2)^2$; the thinner the sample, the faster the transition should be. This can be put to experimental verification; it must be noted that this simple scaling will not be valid for cholesterics and for weakly anchored nematics.

The governing equations (4.1) and (4.2) may be capable of explaining more general situations. So far we have assumed that α or β are changed in small steps. This is equivalent to stating that the magnetic tilt is not a function of time. We can think of a situation where α (or β) is a constant and $\beta = \Omega_\beta t$ (or $\alpha = \Omega_\alpha t$); starting from $t = 0$, **H** from equation (2.2) is rotated at a constant uniform rate. From an experimental viewpoint this would be a generalization of the rotating field experiment discussed in [14]. As long as Ω_α or Ω_β is small enough, equations (4.1) and (4.2) may be able to describe the way the distortion changes in time. Considering complex features such as propagating waves discovered in certain rotating field experiments [20] it appears that when the rate of rotation is high it may be necessary to include the dependence of quantities on other spatial coordinates also; it may also be necessary to add a third component to v and to consider the third component of the force equation which has been ignored here.

4.2. *Stability analysis*

In principle, the transition which occurs at the edge of the bistable region should be studied by explicitly solving equations (4.3) and (4.4) with the boundary conditions from equation (4.5). This is a formidable task as it involves solving a set of coupled non-linear partial differential equations. In the simple one angle description a numerical solution of the problem has been presented [13] by ignoring flow coupling; interestingly, this agrees well with experimental observations.

An alternative approach [14] is to study the stability of the static solution against time dependent perturbations and to find out whether the perturbations have a tendency to grow near the edges of the bistable region. While this approach cannot yield the actual transition time between the states it can still establish that an instability might set in. This has been accomplished in the simple case of twist geometry [14] where flow coupling does not exist in the framework of the assumptions made. It should be interesting to find out whether similar results can be obtained when coupling between orientation and flow fluctuations cannot be neglected. This is attempted below under the rigid anchoring hypothesis.

Consider the static deformation from equation (2.3) under the action of **H** from equation (2.2) satisfying equations (2.6) and (2.8). Let small perturbations θ'', ϕ'' be introduced so that the total deformation is represented by

$$\Theta(z,t) = \theta(z) + \theta''(z,t); \quad \Phi(z,t) = \phi(z) + \phi''(z,t). \tag{4.7}$$

The time variation of θ'', ϕ'' will result in small time dependent stresses σ_{zx}, σ_{zy} which create a velocity perturbation of the form given in equation (4.2). Substituting into equations (4.3) and (4.4), using equations (2.6), (2.8) and (4.5) and linearizing with

respect to the perturbations one obtains the following governing equations and boundary conditions:

$$\left.\begin{aligned}
&f_2(\theta)\theta''_{,zz}+f_5(\theta)\theta_{,z}\theta''_{,z}-f_6(\theta)\phi_{,z}\phi''_{,z}+\theta''[f_5(\theta)\theta_{,zz}\\
&\quad-(\partial f_7/\partial\theta)+\{(df_5/d\theta)\theta^2_{,z}-(df_6/d\theta)\phi^2{}_{,z}\}/2]\\
&\quad-(\partial f_7/\partial\phi)\phi''-\gamma_1\dot\theta''-g_3(\theta,\phi)v_{x,z}-g_6(\theta,\phi)v_{y,z}=0;\\
&f_3(\theta)\phi''_{,zz}+f_6(\theta)\theta_{,z}\phi''_{,z}+f_6(\theta)\phi_{,z}\theta''_{,z}+\theta''[f_6(\theta)\phi_{,zz}\\
&\quad-(\partial f_8/\partial\theta)+(df_6/d\theta)\theta_{,z}\phi_{,z}]-(\partial f_8/\partial\phi)\phi''\\
&\quad-\gamma_1C_\theta^2\dot\phi''+g_4(\theta,\phi)v_{x,z}-g_7(\theta,\phi)v_{y,z}=0;\\
&\sigma_{zx}=g_1(\theta,\phi)v_{x,z}+g_2(\theta,\phi)v_{y,z}+g_3(\theta,\phi)\dot\theta''+g_4(\theta,\phi)\dot\phi''_x=a(t);\\
&\sigma_{zy}=g_2(\theta,\phi)v_{x,z}+g_5(\theta,\phi)v_{y,z}+g_6(\theta,\phi)\dot\theta''+g_7(\theta,\phi)\dot\phi''=b(t);\\
&f_5(\theta)=df_2/d\theta;\quad f_6(\theta)=df_3/d\theta;\quad f_7(\theta,\phi)=\partial f_4/\partial\theta;\quad f_8(\theta,\phi)=\partial f_4/\partial\phi;
\end{aligned}\right\}\tag{4.8}$$

$$(\theta'',\phi'',v_x,v_y)\ (z=\pm h,t)=0.\tag{4.9}$$

Obviously, equations (4.8) and (4.9) represent an eigenvalue problem. The first task is to get the static solution from equations (2.6) and (2.8) at given R, α, β. Then by substituting

$$(\theta'',\phi'',v_x,v_y,a,b)=[\theta''_A(z),\phi''_A(z),v_{xA}(z),v_{yA}(z),a_A,b_A]\exp(\nu t),\tag{4.10}$$

We can get solutions in closed form and also separate variables so that equations (4.8) become a system of ordinary differential equations to be solved with equation (4.9); instead of time dependence, ν enters as a parameter. Solution of equations (4.8) and (4.9) yields a compatibility condition which is satisfied only by discrete values of ν; out of these the highest is chosen. If $\nu<0$ (or if $\nu>0$) the static solution is stable (or unstable).

When $\alpha=0$ and $\theta_\pm=0$ (homogeneous ground state) the variation of β causes **H** to rotate in the xy plane. In this case $\theta(z)=0$ and the static distortion is a pure twist. We get the results which have already been dealt with (see figure 8 of [14]). For the remaining cases it seems advisable to split the discussion into two separate parts.

4.2.1. *Transient splay–bend*

Let $\beta=0$ so that as α is varied **H** rotates in the xz plane. Let there be no superposed twist on the sample: $\phi_0=0$; then , $\phi(z)=0$. The static solution is given by equation (2.8) and

$$f_2(\theta)\theta_{,zz}+\tfrac{1}{2}(df_2/d\theta)\theta^2{}_{,z}-\partial f_4/\partial\theta=0.\tag{4.11}$$

The perturbations $\theta''(z,t)$ and $v_x(z,t)$ get coupled

$$\left.\begin{aligned}
&f_2(\theta)\theta''_{,zz}+f_5(\theta)\theta_{,z}\theta''_{,z}+\theta''[f_5(\theta)\theta_{,zz}-(\partial f_7/\partial\theta)\\
&\quad+\tfrac{1}{2}(df_5/d\theta)\theta^2_{,z}]+\dot\theta''[\{g_3^2(\theta,0)-\gamma_1g_1(\theta,0)\}/g_1(\theta,0)]\\
&\quad=a(t)g_3(\theta,0)/g_1(\theta,0);\\
&\sigma_{zx}=g_1(\theta,0)v_{x,z}+g_3(\theta,0)\dot\theta''=a(t).
\end{aligned}\right\}\tag{4.12}$$

Having obtained $\theta(z)$ at given R and α from equations (4.11) and (2.8), the ansatz $(\theta'',v_x\ a)=[\theta''_A(z),v_{xA}(z),a_A]\exp(\nu_S t)$ is used to calculate the highest eigenvalue ν_{S1} from

equations (4.12) and (4.9). For $\theta_\pm = \theta_1$, this corresponds to the mode (for example mode 1) in which θ_A'' is symmetric and v_{xA} antisymmetric with respect to the sample centre (this symmetry is lost when the director pretilt is more general).

The material parameters are selected from [28]

$$\left.\begin{aligned}&(K_1, K_2, K_3) = (6{\cdot}41, 3{\cdot}97, 9{\cdot}23) \times 10^{-12}\ \text{N};\\&(\mu_1, \mu_2, \mu_3, \mu_4, \mu_5, \mu_6) = (0{\cdot}0, -0{\cdot}0941, -0{\cdot}0045, 0{\cdot}0824, 0{\cdot}0569, -0{\cdot}0417)\ \text{Pa s}.\end{aligned}\right\} \quad (4.13)$$

As μ_1 is generally small its value is taken as zero. The values of the μ_i are so chosen as to satisfy the Parodi relation [4].

Figure 9 (*a*) contains plots of v_{S1} versus α for $\theta_\pm = \pi/2$ (homeotropic anchoring at the boundaries) and three values of R. The corresponding θ_m curves are formally identical

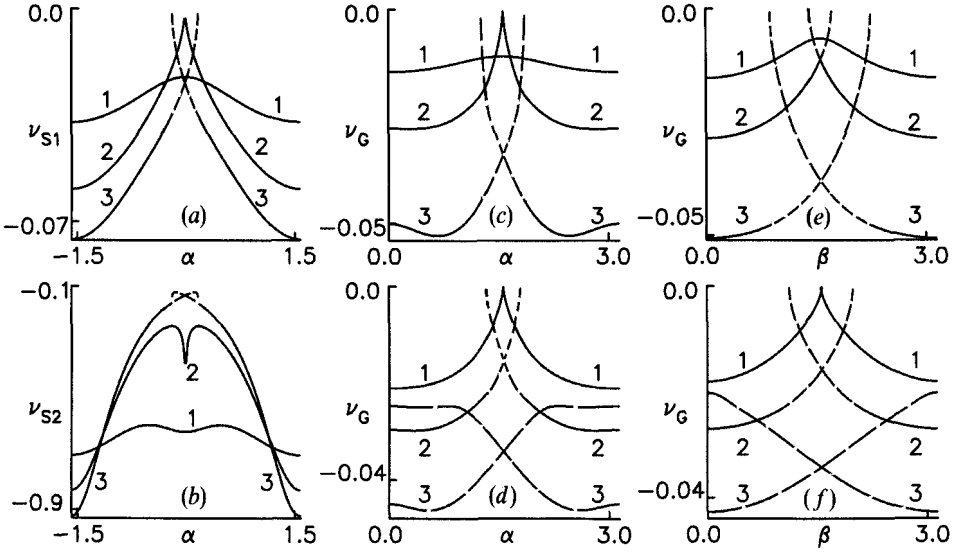

Figure 9. Plots of maximum growth rate (ν) of time dependent linear perturbations versus magnetic tilt angle at different R. Static distortions of types A, B, C are represented. Material parameters are those of equation (4.13) [28]. (*a*) and (*b*) $\theta_\pm = \pi/2$; homeotropic anchoring at the boundaries. $\beta = 0$. **H** rotates in the xz plane when α is varied. $\phi(z) = 0$; single angle description. The static deformation is splay–bend $\theta(z)$. $R = H/H_B$, where $H_B = (\pi/2h)(K_3/\mu_0\chi_a)^{1/2}$ is the bend Freedericksz threshold. Coupling exists between the orientational perturbation θ'' and the velocity perturbation v_x. (*a*) Mode 1; θ'' is even, v_x is odd with respect to the sample centre; v_{S1} versus α. (*b*) Mode 2; θ'' is odd, v_x, is even with respect to the sample centre; v_{S2} versus α. $R = (1)\ 0{\cdot}5\ (2)\ 1{\cdot}0\ (3)\ 1{\cdot}25$. It is sufficient to study mode 1 which always grows faster than mode 2. The v_{S1} curves bear strong resemblance to the F curves of figure 2 (*a*) (see §4.2.1). (*c*)–(*f*) The static distortion is a combination of splay, twist and bend $-\theta(z)$, $\phi(z)$. The perturbations are θ'', ϕ'', v_x, v_y. $R = H/H_F$, where H_F is the splay Freedericksz threshold. $\theta_\pm = 0$ (homogeneous ground state); $\phi_0 = 0$ (no imposed twist). (*c*) and (*d*) v_G versus α for $\beta = (c)\ 0{\cdot}39\ (d)\ 1{\cdot}17$. In (*c*), $R = (1)\ 0{\cdot}5\ (2)\ 1{\cdot}0\ (3)\ 1{\cdot}5$. In (*d*), $R = (1)\ 1{\cdot}0\ (2)\ 1{\cdot}2\ (3)\ 1{\cdot}5$. (*e*) and (*f*) v_G versus β for $\alpha = (e)\ 0{\cdot}05\ (f)\ 1{\cdot}36$. In (*e*), $R = (1)\ 0{\cdot}5\ (2)\ 1{\cdot}0\ (3)\ 1{\cdot}5$. In (*f*), $R = (1)\ 1{\cdot}0\ (2)\ 1{\cdot}2\ (3)\ 1{\cdot}5$. It is seen that type A and type C distortions are stable over the entire range of magnetic tilt. The type B static deformation shows a propensity towards instability as the magnetic tilt approaches the edges of the bistability region. Observe the shape similarity between the v_G curves and the F curves of figure 2 (see §4.2.2); see also [14].

to those of figure 1 (*a*). At $R=0{\cdot}5$ (curve 1), v_{S1} remains negative showing that $\theta(z)$ is stable throughout the α range. When $R=1{\cdot}25$ (curves 3), v_{S1} increases from a negative value as α is varied from the limits of its range; $v_{S1}\to 0$ as α approaches the edges of the bistable region where the static solution has a propensity to undergo instability. Interestingly, for $R=1{\cdot}0$ (curve 2) the variation of v_{S1} is sharp at $\alpha=0$ and v_{S1} is also close to zero. Hence we cannot rule out a small jump in the distortion as α crosses the middle of the range. There also exists a similarity between the F and v_{S1} curves (compare with figure 2).

It is possible to investigate the other uncoupled mode (mode 2) which has symmetry opposite to that of mode 1. Figure 9 (*b*) contains a plot of the inverse rise time v_{S2} as a function of α; clearly, mode 2 is of no interest as it always damps out faster than mode 1.

4.2.2. *General transient dynamics*

Suppose the tilt of **H** is changed in a general way. Then the static distortion $\theta(z)$, $\phi(z)$ is given by equations (2.6) and (2.8). To solve equations (4.8) and (4.9) for the perturbations, we use the ansatz from equation (4.10) to solve for the velocity gradients:

$$\left.\begin{aligned}
&dv_{xA}/dz = L_1 a_A + L_2 b_A + L_3 v\theta'' + L_4 v\phi'';\\
&dv_{yA}/dz = L_5 a_A + L_6 b_A + L_7 v\theta'' + L_8 v\phi'';\\
&\Delta = g_2^2 - g_1 g_5;\quad L_1 = -g_5/\Delta;\quad L_2 = L_5 = g_2/\Delta;\quad L_3 = (g_3 g_5 - g_2 g_6)/\Delta;\\
&L_4 = (g_4 g_5 - g_2 g_7)/\Delta;\quad L_6 = -g_1/\Delta;\quad L_7 = (g_1 g_6 - g_2 g_3)/\Delta;\\
&L_8 = (g_1 g_7 - g_2 g_4)/\Delta.
\end{aligned}\right\} \tag{4.14}$$

Obviously, the L_i and Δ are functions of $\theta(z)$ and $\phi(z)$. Integrating the velocity gradients with respect to z and using the boundary conditions from equation (4.9) expressions can be obtained connecting the indeterminate stress amplitudes a_A, b_A implicitly in terms of the perturbations θ'', ϕ'';

$$\left.\begin{aligned}
&a_A = v\int\theta'' P_1 dz + v\int\phi'' P_2 dz;\quad b_A = v\int\theta'' P_3 dz + v\int\phi'' P_4 dz;\\
&I_1 = \int L_1 dz;\quad I_2 = \int L_2 dz;\quad I_5 = \int L_5 dz;\quad I_6 = \int L_6 dz;\quad \Delta_I = I_1 I_6 - I_2 I_5;\\
&N_1 = I_1/\Delta_I;\quad N_2 = I_2/\Delta_I;\quad N_5 = I_5/\Delta_I;\quad N_6 = I_6/\Delta_I;\\
&P_1 = L_7 N_2 - L_3 N_6;\quad P_2 = L_8 N_2 - L_4 N_6;\\
&P_3 = L_3 N_5 - L_7 N_1;\quad P_4 = L_4 N_5 - L_8 N_1;
\end{aligned}\right\} \tag{4.15}$$

all integrals in these equations are from $z=-h$ to $z=+h$. It is worth noting that the integrals P_i are dependent only on the static solution. By substituting for a_A, b_A from

equation (4.15) into equations (4.14) and (4.8) a pair of integro-differential equations are obtained for θ''_A, ϕ''_A to be solved with equation (4.9):

$$\left.\begin{aligned}
&f_2(\theta)\theta''_{A,zz}+f_5(\theta)\theta_{,z}\theta''_{A,z}-f_6(\theta)\phi_{,z}\phi''_{A,z}\\
&\quad-[(\partial f_7/\partial\phi)+\nu M_4(\theta,\phi)]\phi''_A+\theta''_A[f_5(\theta)\theta_{,zz}\\
&\quad-(\partial f_7/\partial\theta)+\tfrac{1}{2}\{(df_5/d\theta)\theta^2_{,z}-(df_6/d\theta)\phi^2_{,z}\}\\
&\quad-\nu M_3(\theta,\phi)]-a_A M_1(\theta,\phi)-b_A M_2(\theta,\phi)=0;\\
&f_3(\theta)\phi''_{A,zz}+f_6(\theta)(\theta_{,z}\phi''_{A,z}+\phi_{,z}\theta''_{A,z})-(\partial f_8/\partial\phi)\phi''_A\\
&\quad+\nu M_8(\theta,\phi)\phi''_A+\theta''_A[f_6(\theta)\phi_{,zz}-(\partial f_8/\partial\theta)\\
&\quad+(df_6/d\theta)\theta_{,z}\phi_{,z}+\nu M_7(\theta,\phi)]+a_A M_5(\theta,\phi)+b_A M_6(\theta,\phi)=0;\\
&M_1=g_3L_1+g_6L_5;\quad M_2=g_3L_2+g_6L_6;\quad M_3=\gamma_1+g_3L_3+g_6L_7;\\
&M_4=g_3L_4+g_6L_8;\quad M_5=g_4L_1-g_7L_5;\quad M_6=g_4L_2-g_7L_6;\\
&M_7=g_4L_3-g_7L_7;\quad M_8=g_4L_4-g_7L_8-\gamma_1C^2_\theta.
\end{aligned}\right\}\tag{4.16}$$

By using the orthogonal collocation method in tandem with the gaussian quadrature integration formula, these equations can be translated into a set of coupled linear equations whose compatibility condition can be used to obtain the highest eigenvalue ν_G of ν for different magnetic tilt angles and reduced field (see figures 9 (*c*)–(*f*)).

The following features may be noted. When R is low enough, the static solution is stable for all magnetic tilts. When R is high and the static distortion shows type C behaviour, $\nu_G<0$ for all magnetic tilts. The static solution shows a tendency towards destabilization ($\nu_G\to0$) as the magnetic tilt approaches the edges of the region of bistability when the distortion conforms to type B variation. The shape similarities between the ν_G curves and the corresponding F curves (see figures 2 (*a*)–(*d*)) can be noted.

5. Conclusions

An attempt has been made to generalize the theoretical work of [11–14] to study the nature of change of deformation with magnetic tilt angle when **n** is described to two angles. Quite a few of the predictions can be put to experimental test. The results for $\chi_A>0$ become similar to those of [11–14] when **H** rotates in a plane which is either close to the sample boundaries ($\alpha\approx0$) or normal to them ($\beta=0$) with **n** being initially uniformly aligned in the magnetic plane; in this case the distortion shows either type A (continuous variation with magnetic tilt without bistability) or type B (bistability associated with discontinuous variation at the edges of the bistable region) behaviour. When the magnetic plane is sufficiently tilted with respect to the sample boundaries a new kind of variation (type C) is found when the field is strong enough; the deformation changes continuously over the entire range of magnetic tilt with bistability. It is possible to account for these results in terms of energy flow between the splay–bend and the twist modes of distortion.

Even for general orientations of **H**, the deformation changes symmetrically when the magnetic tilt is varied from the two ends of its range for the homogeneous ground state. When the ground state is uniformly pretilted it is found that the distortion changes by different extents for the two different variations of magnetic tilt. This

appears to be due to the different ways in which twist can couple with splay–bend near the two ends of the magnetic tilt when the ground state has a uniform pretilt.

The viewpoint adopted in [14] has been extended to the present case to study the stability of the static deformation against time dependent perturbations; only the homogeneous untwisted ground state is considered. It is found that type A and type C solutions are stable over the entire range of magnetic tilt; the type B solution shows a propensity towards instability as the magnetic tilt approaches the edges of the bistable region. It should be instructive to extend this study to more general cases such as the uniformly pretilted ground state.

Scaling analysis of the static equations shows that when anchoring is rigid the bistability width (relevant to type B variation of deformation) for a given nematic should be independent of the sample thickness at a fixed reduced field; this scaling, which breaks down for a nematic when the anchoring is not rigid, does not also exist for a cholesteric. Scaling analysis of the dynamical equations shows that the time of transition should strongly depend on the sample thickness at the same reduced field—the thinner the sample, the faster the transition. The importance of adjusting the transition time by changing sample thickness becomes clear when we discuss certain other ramifications of the dynamical effect later in this section.

The case of a $\chi_a < 0$ nematic has been briefly treated. For the homogeneous ground state a striking qualitative difference can be observed between this case and that of the $\chi_a > 0$ nematic. For the $\chi_a < 0$ case, type B behaviour is found only for β variation at a given α; type C behaviour does not seem to exist. For the α variation (at fixed β) one finds only type A behaviour. When the magnetic plane is normal to the sample boundaries and also contains the splay–bend deformation ($\beta = 0$) there appears to be a threshold polar angle α_C; when α is varied beyond α_C an additional twist component can appear when H is high enough. It is possible to estimate α_C by linear (time independent) perturbation analysis. Similarly one can find a threshold for transition from the twist via splay–bend perturbations when **n** and **H** are initially confined to the same plane parallel to the sample boundaries. This brief foray indicates that a more detailed study of the $\chi_a < 0$ case should be worthwhile.

As long as the ground state is uniformly tilted the distortion at any H for any magnetic tilt will be symmetric with respect to the sample centre. This is not true when the ground state has an imposed twist; the deformation becomes asymmetric. In spite of this the nature of variation of the distortion for a given ground state twist turns out to be similar to that of the untwisted case. To show this results have been briefly presented for twisted nematics with different ground state twists. It is possible to obtain ground states with different twists by using chiral impurities [5]. With an additional pretilt it seems possible to get super twisted structures [25]. It appears reasonable to postpone a detailed study of these cases to the future with particular reference to a comparison with the simple twisted case. In particular, it should be instructive to find out how the nature of variation of distortion is affected when the material has $\chi_a < 0$.

The case of a cholesteric has been mentioned in passing mainly to show additional complications that may arise. When the ground state pitch is sufficiently small a homogeneous distortion may not be energetically feasible for certain tilts of **H**; we can expect periodic deformations [29]. It should be interesting to investigate the nature of variation of deformation for different pitches. From the experimental viewpoint it should be possible to find out whether periodic and non-periodic (homogeneous) distortions occur in different ranges of magnetic tilt angles. Even when the deformation is homogeneous the intrinsic twist of the cholesteric can be expected to affect the range

and occurrence of bistability. Due to the additional intrinsic twist term in the free energy density, the distortion will also be asymmetrical for most values of the magnetic tilt angles.

In the case of the single angle description [14] it has been shown that the very occurrence of bistability can be controlled by the application of an additional **E** along different directions; for type B variation in particular the bistability width can be influenced by **E**. Naturally factors such as the sign of the dielectric anisotropy ϵ_a and the boundary conditions are important in determining how much the electric field inside the sample gets influenced by the distortion. It has not been possible to take account of **E** in the present communication; however some qualitative features of the effect of **E** can be discussed. For a nematic with $\epsilon_a > 0$, **E** applied normal to the sample boundaries reduces the magnetic splay Freedericksz threshold; this should increase R at a given value of H. But when the ground state is homeotropic **E** can actually enhance the bend magnetic Freedericksz threshold. Hence **E** can have a stabilizing or a destabilizing influence depending upon the initial pretilt of the ground state.

It has been shown [30] that the effect of **E** applied parallel to the sample planes can be quite complicated especially because the peculiar nature of its modification by the presence of distortions leads to a discontinuous electric bend Freedericksz transition. In the present context of general director deformations **E**, applied along the sample boundaries, assumes special importance because it can be impressed along various directions. The effects of an additional electric field will be treated elsewhere.

Finally mention must be made of possible generalizations of the static limit to include dynamic effects. One of the simplest in this category is the rotating magnetic field. As noted earlier [16–20] a variety of interesting results have been found when a nematic sample is subjected to a rotating **H**. In an earlier communication [14] it had been indicated that a rotating field (or sample) experiment should serve as the dynamical analogue of the static experiments already reported in [11, 13] on director deformations described by a single degree of freedom. It may be worth elaborating this a little in the light of results obtained here. As the scaling analysis makes it clear, the time of transition at the edge of the bistable region should strongly depend on the sample thickness. By adjusting the sample thickness it may be possible to make this time coincide with the rotation period; this might lead to the observation of resonance. Theoretical results of this work make it clear that generalizations of such experiments to include variations in the axis of rotation of field (or sample) should prove fruitful.

The author thanks a referee for useful comments on an earlier version of this work.

References

[1] OSEEN, C. W., 1933, *Trans. Faraday Soc.*, **29**, 883.
[2] FRANK, F. C., 1958, *Discuss Faraday Soc.*, **25**, 19.
[3] ERICKSEN, J. L., 1976, *Advances in Liquid Crystals*, edited by G. H. Brown (Academic Press), p. 233.
[4] LESLIE, F. M., 1979, *Advances in Liquid Crystals*, edited by G. H. Brown (Academic Press), p. 1. PARODI, O., 1970, *J. Phys. Paris*, **31**, 581.
[5] DE GENNES, P. G., 1974, *The Physics of Liquid Crystals* (Clarendon Press), Chaps 3 and 5.
[6] DEULING, H. J., 1978, *Solid St. Phys. Suppl.*, **14**, 77.
[7] CHANDRASEKHAR, S., 1977, *Liquid Crystals* (Cambridge University Press), Chap. 3.
[8] BLINOV, L. M., 1983, *Electro-optical and Magneto-optical Properties of Liquid Crystals* (John Wiley), Chaps 3 and 4.

[9] BROCHARD, F., 1973, *Molec. Crystals liq Crystals*, **23,** 51. PIERANSKI, P., BROCHARD, F., and GUYON, E., 1973, *J. Phys. Paris*, **34,** 35.
[10] SRAJER, G., FRADEN, S., and MEYER, R. B., 1989, *Phys. Rev.* A, **39,** 4828 and references therein.
[11] ONNAGAWA, H., and MIYASHITA, K., 1974, *Jap. J. appl. Phys.*, **13,** 1741.
[12] MOTOOKA, T., and FUKUHARA, A., 1979, *J. appl. Phys.*, **50,** 3322.
[13] KARN, A. J., and SHEN, Y. R., 1990, *Phys. Rev.* A, **41,** 4510.
[14] KINI, U. D., 1991, *Liq. Crystals*, **10,** 597.
[15] RAPINI, A., and PAPOULAR, M., 1969, *J. Phys. Colloq., Paris*, **30,** C4–54. GUYON, E., and URBACH, W., 1976, *Non-emissive Electro-optic Displays*, edited by A. R. Kmetz and F. K. von Willisen (Plenum Press), p. 121.
[16] GASPAROUX, H., and PROST, J., 1971, *J. Phys. Paris*, **32,** 65.
[17] LESLIE, F. M., LUCKHURST, G. R., and SMITH, H. J., 1972, *Chem. Phys. Lett.*, **13,** 368.
[18] BROCHARD, F., LEGER, L., and MEYER, R. B., 1975, *J. Phys. Colloq., Paris*, **36,** C1–209. SAGUES, F., 1988, *Phys. Rev.* A, **38,** 5360.
[19] HORNREICH, R. M., 1977, *Phys. Rev.* A, **15,** 1767. YO, C. H., POUPKO, R., and HORNREICH, R. M., 1978, *Chem. Phys. Lett.*, **54,** 142.
[20] MIGLER, K. B., and MEYER, R. B., 1991, *Phys. Rev. Lett.*, **66,** 1485.
[21] LESLIE, F. M., 1970, *Molec. Crystals Liq. Crystals*, **12,** 57; 1969, *Ibid.*, **7,** 407.
[22] FINLAYSON, B. A., 1972, *The Method of Weighted Residuals and Variational Principles* (Academic Press), Chap. 5. TSENG, H. C., SILVER, D. L., and FINLAYSON, B. A., 1972, *Phys. Fluids*, **15,** 1213.
[23] ABRAMOWITZ, M., and STEGUN, I. A. (editors), 1972, *Handbook of Mathematical Functions* (Dover).
[24] BERREMAN, D. W., 1980, *The Physics and Chemistry of Liquid Crystal Devices*, edited by G. J. Sprokel (Plenum Press) p. 1.
[25] BERREMAN, D. W., and HEFFNER, W. R., 1981, *J. appl. Phys.*, **52,** 3032. WATERS, C. M., RAYNES, E. P., and BRIMMEL, V., 1985, *Molec. Crystals, liq. Crystals*, **123,** 303.
[26] It is only in the linear limit that θ'' and ϕ'' get uncoupled. Once the perturbation has developed sufficiently the total deformation will be given by equations (2.3) and (2.6); equation (2.6) has been derived without making assumptions about the magnitudes of the distortions. Equations (3.13) and (3.17) and their solutions presented in figure 8 are valid only for determining the thresholds α_C and β_C.
[27] PORTE, G., 1976, *J. Phys., Paris*, **37,** 1245. BOYD, G. D., CHENG, J., and NGO, P. D. T., 1980, *Appl. Phys. Lett.*, **36,** 556.
[28] CHEN, G.-P., TAKEZOE, H., and FUKUDA, A., 1989, *Liq. Crystals*, **5,** 341.
[29] HELFRICH, W., 1971, *J. chem. Phys.*, **55,** 839. RONDELEZ, F., and HULIN, J. P., 1972, *Solid St. Commun.*, **10,** 1009.
[30] FRISKEN, B. J., and PALFFY-MUHORAY, P., 1989, *Phys. Rev.* A, **39,** 1513; **A40,** 6099. KINI, U. D., 1990, *Liq. Crystals*, **8,** 745.